

A Review of Dynamic Phasor Estimation by Non-Linear Kalman Filters

JALAL KHODAPARAST¹

Department of Electrical Engineering, IT and Cybernetic, University of South-Eastern Norway (USN), 3918 Porsgrunn, Norway

e-mail: jalal.khodaparast@usn.no

ABSTRACT Phasor estimation under dynamic conditions has been under study recently by relaxing the amplitude and phase of the static phasor. This paper will review some methods to estimate dynamic phasor by nonlinear Kalman filters. Nonlinear Kalman filters have found an application in the tracking of time-varying amplitude and phase. Five nonlinear Kalman filtering methods for dynamic phasor estimation are examined in this paper. These methods are: EKF1 stands for first-order Extended Kalman filter, EKF2 stands for second-order Extended Kalman, UKF stands for Unscented Kalman filter, GHKF stands for Gauss Hermite Kalman filter, and finally CKF stands for Cubature Kalman filter. This paper describes the theoretical processes of these methods and demonstrates their effectiveness in dynamic phasor estimation by some test signal simulations in MATLAB. The simulation section shows that nonlinear Kalman filters give more accuracy than linear Kalman filters when the phasor is relaxed by modulated amplitude and phase. Moreover, comparative assessments among the performance of five nonlinear Kalman filters are done for dynamic phasor estimation, and also their performances are compared with the other methods which have already been published. According to the simulation results, EKF1 gives the highest accuracy during steady-state (2×10^{-13}) because the signal model is more similar to the estimation model of EK1 during the steady-state condition. However, the other non-linear Kalman filters show better performances in dynamic conditions. When the phasor is a time-varying amplitude and phase, filters give the same accuracy ($TVE = 0.5\%$). A step-change in amplitude and phase creates different overshoot and response times, but EKF2 shows the least overshoot (3.2%) and the longest response time (7.6 ms). Computation burden and noise indices can discriminate the methods from other viewpoints. The computation burden of GHKF is drastically increased when the number of states gives rise. CKF shows an appropriate performance when the number of samples and the number of the state increased in the input signal. EKF1 is not a good solution for noise infiltration when SNR is less than 40 dB, but CKF gives the highest accuracy in high noise levels. Compared to the six already published methods, CK shows the best performance with a reasonable estimation error ($TVE = 0.1101\%$) and simulation time (0.6146 ms).

INDEX TERMS Dynamic phasor, non-linear Kalman filter, phasor estimation, wide area protection.

I. INTRODUCTION

The complexity of modern power systems is steadily increasing. It is inspiring for researchers to address several challenges of modern power systems. Power system dynamics vary significantly by huge penetrations of renewable energy, so it demands new platforms to monitor the power system. Phasor measurement units (PMUs) as a synchronized monitoring system presents a reliable platform for the complicated power system [1], [2]. Various signal analysis techniques can be employed to estimate applicable parameters of the

measured signal by the PMU, such as Least square, Wavelet transform, Kalman filters, Hilbert-Huang Transform, and Prony [3].

There are two main standards for phasor estimation in phasor estimation unit (PMU) (IEC/IEEE 60255-118-1 published in 2018 and IEEE C37.118.1 published in 2011) that have constructed a framework and covered issues from phasor estimation to communication. In the standards, several dynamic test signals (such as modulation, frequency ramp, and signal parameters jumps) are recommended for the performance evaluation under dynamic conditions (where the signal parameters (i.e., amplitude, phase, and frequency) of the input signal are not fixed and change during time).

The associate editor coordinating the review of this manuscript and approving it for publication was Halil Ersin Soken².

Dynamic phasor is a new notion that can improve accuracy of estimation under dynamic conditions and more studies should be done for clarification [4], [5]. Dynamic phasor application is not limited to PMU, and it is also profitable in simulation programs [6]. There are two domains of simulation in the simulation program; time domain and phasor domain. Time-domain needs a complete model of components and solving system variables in every sample, which requires a long simulation time. However, in the phasor-domain, phasor of system variables are used, which reduces simulation time significantly. Nowadays, the phasor-domain methods of simulation programs are based on a static phasor, which considers phasor a fixed amplitude and phase. This unreal concept of phasor faces difficulties in solving systems containing modern devices like FACTS. The dynamic phasor notion proposed in [7] can improve the accuracy of simulation cases when there is a dynamic condition in the power system simulations.

The phasor estimation block as an internal part of the PMU can be driven by different algorithms [5], [8]. Some of the recent publications consider the following topics: Maximum likelihood algorithm based on a semi-orthogonal transform to estimate phasor with lower computation complexity [9], Robust DFT-based technique to estimate phasor when DC component is in the measured signal by PMU [10], Dictionary matrix to estimation procedure for low-cost estimation in a P-class PMU [11], Modified Gauss-Newton adaptive filter estimated time varying-phasor of the fundamental component [12], Recursive wavelet transform to estimate the phasor only by a quarter cycle of the measured signal [13], Shank method, which is widely used in designing a digital filter, to estimate the phasor [14]. Methods have pros and cons in terms of delay, noise, computation burden, integer and non-integer harmonics, off-nominal frequency.

By relaxing the amplitude and phase of the static phasor, a new notation is formed, which is called dynamic phasor. In a quasi-steady-state condition, the amplitude and phase of the main signal are not fixed and may change during time. This phenomenon is observed in the power systems when there is a power swing (stable or unstable) consequence of a range of events. Sudden loss of generation, severe sort circuit (faults), and sudden connecting and tripping of large loads are some examples of roots of power swing [15], [16]. As a result of these phenomena, the flow of power will fluctuate, creating problems for the protection system (distance relay) and phasor estimation in PMUs. The topic of dynamic phasor estimation has been studied in different references. Prony algorithm is a promising method presented in [17] to estimate dynamic phasor when the frequency of the system is also changing with time. The saturation problem created by the current transformer is solved by the proposed method in [18], in which phasor estimation is done by a least square-based curve fitting. The instantaneous phasor is calculated by the angle-shifted-based energy, which is proposed in [19]. Kalman filter as an instantaneous estimator combined with Taylor expansion has application in dynamic

phasor estimation as shown in [20], [21]. A combination of Taylor expansion and Least-square technique as a one-cycle-delay estimator is used in dynamic phasor estimation, and the results of the method are presented in [22]. Adaptive band-pass filter presented in [23] is another promising method is phasor estimation. DC offset issue in phasor estimation procedure is resolved in [24] by applying a new modified Fourier Transform. More methods and more elaborations about phasor estimation under steady-state and dynamic conditions can be found in references [25]–[30].

Kalman filter-based algorithms are extensively employed to estimate and track the parameters [31]. Little computation burden, instantaneous (Zero delays) estimation by a recursive algorithm makes the Kalman filter a promising observer [32]. Kalman filters combine two sources of information, the predicted states and noisy measurements, to produce optimal, unbiased estimates of system states. The filter is optimal in the sense that it minimizes the variance in the estimated states. Kalman filter is statistically optimal in a sense that it gives the minimum error covariance estimate, based on all available observation data at the present time step under the linear system. A Kalman filter (linear or non-linear) is generally based on a dynamic state-space model, representing the movement of a system's desired states in the time domain. An estimation is accomplished by the Kalman filter in two steps. The estimates are predicted in the first step by a mathematical model and the last estimates. The predicted estimates in the first step will be adjusted in the second step by a feedback loop. The Kalman filter modifies the predicted estimates by remedial term. The remedial term is a subtraction of the measured signal by the estimated signal that is weighted by a Kalman filter gain [33], [34]. Kalman filtering has been extensively applied to many areas, but we concentrate on its applications to power system signal frequency and phasor estimation. Extended Kalman filter (EKF) has been widely used to track and estimate the frequency as presented in [35]–[37]. [38] has dealt with the inter-harmonic issue by a new method based on a mixture of Kalman filter and CSTFM. In [39], Kalman filter and output smoother is utilized to improve the accuracy of estimation. An extended Kalman filter based on generalized state-space model is proposed in [40] to estimate the frequency of harmonic components with a noisy measurement. Phase angle and consequently the frequency is estimated by the method proposed in [41] based on a complex data linear Kalman filter. An improved UKF is proposed in [42] to estimate the harmonics and frequency of the main signal when the signal is changing during time. [43] and [44] are other references which concentrate on frequency tracking by Kalman filter.

The application of the linear Kalman filter may be complex in real-world issues because a steady-state model and measurement model of a dynamic system are usually non-linear [45]. One of these nonlinear systems is the phasor estimation system. The Nonlinear Kalman filter is proposed here as a nonlinear and instantaneous estimator. However, there are several kinds of literature related to the algorithms

of dynamic phasor estimation and nonlinear Kalman filter applications for frequency tracking individually, but nonlinear Kalman filter has not gotten attention in dynamic phasor estimation. This paper aims to compare performance of nonlinear Kalman filters in dynamic phasor estimation that can be used mostly in PMU (class M and class P) and phasor estimation used in a distance relay. Designing algorithms of five nonlinear Kalman filters for nonlinear phasor estimation are presented in this paper. These five methods are:

A) EKF1 method: This algorithm approximates the nonlinear function by a fifth-order Taylor expansion [46].

B) EKF2 method: Second-order Taylor expansion has been used to approximate non-linear function in this method [46].

C) UKF method: One of the main concerns of the first two methods is the derivative of a nonlinear function. Compared with the second method, the UKF method uses Unscented Transformation (UT) to solve this problem. The process and observation models are considered a black box in this method [46], [47]. The fundamental part of this method is the UT which utilizes a collection of weighted points to calculate the averages and covariances of distributions.

D) GHKF method: the main design of this method is the use of the Gauss Hermite algorithm for calculating integral numerically [48]. The main challenge in GHKF design is related to the number of sigma points which rises exponentially with increasing dimension number [46].

E) CKF method: spherical radial method is used in this method to calculate integral. This method is actually a kind of UKF with specific parameters [46], [48].

The mathematical foundation of Non-linear Kalman filters is not author's contribution. It has been tried to form a state-space model of non-linear Kalman filter for dynamic phasor estimation and implement non-linear Kalman filters to estimate a dynamic phasor. Application of non-linear Kalman filter in dynamic phasor estimation is the contribution of this paper. We collect and compare different types of filters to enrich this paper to be helpful to electrical power engineers to use these filters in future monitoring systems. There are different types of non-linear Kalman filters in the literature. Methods are selected from extended category (EKF1 and EKF2), black box category (UKF) and numerical integration solver (GHKF and CKF) to cover problem of dynamic phasor estimation from different viewpoints. This paper aims to investigate the performance of five different nonlinear Kalman filters for estimation of the dynamic phasor. The principal contributions of this review paper are:

- Presenting methodological stages of nonlinear Kalman filters.
- Formulation of state space of dynamic phasor estimation which is used by nonlinear Kalman filters.
- Comparison of linear and nonlinear Kalman filters when amplitude and phase of the main signal are time varying.
- Comparison of the performance of different nonlinear Kalman filters for dynamic phasor estimation.

- Comparison of performance of nonlinear Kalman filters with some other methods which have already been published.

The paper is arranged as follows: Section II presents the methodological stages of five nonlinear Kalman filters. The formulation of state-space for dynamic phasor estimation by nonlinear Kalman filters is presented in Section III. Section IV presents simulation results to verify the analytical achievements. Steady-state compliance, dynamic compliance (bandwidth and step change), electrical power system case, IEEE 39 Bus simulation in DlgSILENT, noise, computation burden, and comparison with other dynamic phasor estimation methods are subsections included in section IV. Section V concludes the research, and section VI presents the future work.

II. NON-LINEAR KALMAN FILTERS

Since system dynamics and observation equations of most interesting applications are nonlinear, estimating the state of such a system is not accurate if linear Kalman filter is used for estimation process [49]. In these kinds of systems, one or both dynamic and measurement models may be nonlinear. A dynamic model of a nonlinear discrete-time system has the form of:

$$x_k = f(x_{k-1}) + q_{k-1} \quad (1)$$

where f is a nonlinear dynamic model function, x_k is the state of the system, k is counter of step-time, and q_{k-1} is the process noise originated by modeling error. q_{k-1} stands for normal distribution with mean value of zero and variance value of Q_{k-1} .

$$y_k = h(x_k) + r_k \quad (2)$$

where h is the nonlinear measurement model function, y_k is the measurement, and r_k is the measurement noise. r_k stands for normal distribution with mean value of zero and variance value of R_k . Since the Kalman filter was proposed, researchers have continuously developed various improvements to this algorithm. First-order and second-order extended Kalman filter, unscented Kalman filter, Gauss Hermite Kalman filter, and cubature Kalman filter are different nonlinear Kalman filters which are proposed in the literature. The methodological stages of these five nonlinear Kalman filters are presented in this section.

A. FIRST ORDER EXTENDED KALMAN FILTER (EKF)

Extended Kalman filter (EKF) is one derivation of Kalman filter for optimally estimating the states and parameters of nonlinear systems based on first-order and second-order linearization [50]. The Extended Kalman filter expands the principle of Kalman filter to nonlinear optimal filtering using Taylor series-based transformation. The advantage of the EKF is that it answers the nonlinear equations while granting optimal denoising [51]. If just two parameters of Taylor series expansion are used, this Kalman filter would be First-Order Extended Kalman Filter (EKF1). The extended Kalman filter

is also divided into two stages, just like the linear Kalman filter. The future state of the system is predicted by the process model. Mean value of state is predicted as:

$$m^- = f(m_{k-1}) \quad (3)$$

where m_{k-1} is the mean of last estimate at step time k before observing the measurement. The predicted covariance of state is:

$$P^- = F_x(m_{k-1}).P_{k-1}.F_x^T(m_{k-1}) + Q_{k-1} \quad (4)$$

where P_{k-1} is the covariance of last estimate at step time k , and matrix F_x is the Jacobian of nonlinear model function f represented by:

$$F_x = \left[\frac{\partial f}{\partial x_1}, \frac{\partial f}{\partial x_2}, \dots, \frac{\partial f}{\partial x_n} \right] \quad (5)$$

The corrected mean and covariance of estimate is given by updating the prediction with the current sensor measurement as follows:

$$m = m^- + K.v \quad (6)$$

$$P = P^- - K.S.K^T \quad (7)$$

where m and P are the estimated mean and covariance of the state, respectively, on time step k after observing the measurement. Sign “.” represents a mathematical product operator. v is the measurement residual and calculated by:

$$v = y - h(m^-) \quad (8)$$

In (6) and (7), capital letter K was gain of Kalman filter (tells the correction amount in the prediction) and calculated as:

$$K = P^- .H_x^T(m^-)/S \quad (9)$$

where S is the measurement prediction covariance given by

$$S = H_x(m^-).P^- .H_x^T(m^-) + R_k \quad (10)$$

where matrix H_x is the Jacobian of nonlinear measurement function h

$$H_x = \left[\frac{\partial h}{\partial x_1}, \frac{\partial h}{\partial x_2}, \dots, \frac{\partial h}{\partial x_n} \right] \quad (11)$$

It is worthy to note that EKF1 is a suboptimal nonlinear filter since this filter delivers the first-order accuracy by ignoring the higher-order terms in Taylor’s series expansion [52]. The whole estimation procedure of EKF1 is shown in Fig. 1.

B. SECOND ORDER EXTENDED KALMAN FILTER (EKF2)

The difference between the first-order and second-order extended Kalman filter is in utilizing the higher terms in the Taylor series. The first three terms of Taylor series expansion (second-order expansion) are used in this method). The processes which occur in EKF2 consists of prediction step and updating step. In the prediction step, the mean value of state is predicted based on previous estimates as:

$$m^- = f(m_{k-1}) + \frac{1}{2}trace\{F_{xx}(m_{k-1}).P_{k-1}\} \quad (12)$$

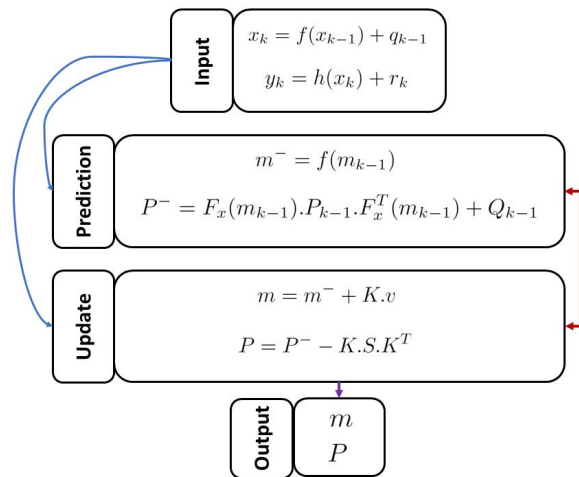


FIGURE 1. Flowchart of EKF1.

where compared to EKF1 presented in(3), new term is added to the prediction. “trace” extracts the diagonal elements and adds them together in the partial derivative function F_{xx} presented in (13).

$$[F_{xx}] = \begin{bmatrix} \frac{\partial^2 f}{\partial x_1 \partial x_1} & \frac{\partial^2 f}{\partial x_1 \partial x_2} & \dots & \frac{\partial^2 f}{\partial x_1 \partial x_n} \\ \frac{\partial^2 f}{\partial x_2 \partial x_1} & \frac{\partial^2 f}{\partial x_2 \partial x_2} & \dots & \frac{\partial^2 f}{\partial x_2 \partial x_n} \\ \vdots & \vdots & \ddots & \vdots \\ \frac{\partial^2 f}{\partial x_n \partial x_1} & \frac{\partial^2 f}{\partial x_n \partial x_2} & \dots & \frac{\partial^2 f}{\partial x_n \partial x_n} \end{bmatrix} \quad (13)$$

Predicted covariance of estimate is calculated by EKF2 by (14).

$$P^- = F_x(m_{k-1}).P_{k-1}.F_x^T(m_{k-1}) + Q_{k-1} + \frac{1}{2}trace\{F_{xx}(m_{k-1}).P_{k-1}.F_{xx}(m_{k-1}).P_{k-1}\} \quad (14)$$

The predicted mean and covariance are used in the updating step to be modified. The updated mean value is:

$$m = m^- + K.v \quad (15)$$

and updated covariance is:

$$P = P^- - K.S.K^T \quad (16)$$

where the Kalman filter’s gain K , v and S are calculated respectively by equations (17), (18), and (19).

$$K = P^- .H_x^T(m^-)/S \quad (17)$$

$$v = y - h(m^-) - \frac{1}{2}trace\{H_{xx}^i(m^-).P^-\} \quad (18)$$

$$S = H_x(m^-).P^- .H_x^T(m^-) + R_k + \frac{1}{2}trace\{H_{xx}^i(m^-).P^- .H_{xx}^i(m^-).P^-\} \quad (19)$$

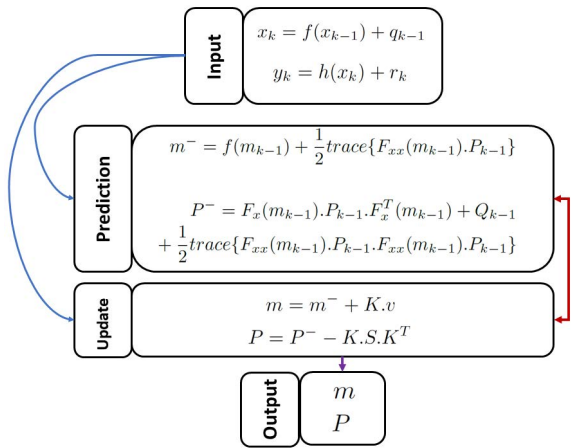


FIGURE 2. Flowchart of EKF2.

where matrix H_{xx} is partial derivative of nonlinear function of measurement and expressed as:

$$[H_{xx}] = \begin{bmatrix} \frac{\partial^2 h}{\partial x_1 \partial x_1} & \frac{\partial^2 h}{\partial x_1 \partial x_2} & \cdots & \frac{\partial^2 h}{\partial x_1 \partial x_n} \\ \frac{\partial^2 h}{\partial x_2 \partial x_1} & \frac{\partial^2 h}{\partial x_2 \partial x_2} & \cdots & \frac{\partial^2 h}{\partial x_2 \partial x_n} \\ \vdots & \vdots & \ddots & \vdots \\ \frac{\partial^2 h}{\partial x_n \partial x_1} & \frac{\partial^2 h}{\partial x_n \partial x_2} & \cdots & \frac{\partial^2 h}{\partial x_n \partial x_n} \end{bmatrix} \quad (20)$$

According to required derivative matrices, two presented methods (EKF1 and EKF2) need linearization, which introduces significant errors in many practical situations. The EKF1 and EKF2 are also challenging to be realized since the calculations of Jacobian matrices require high computation capacity in a complex system. It is worthy to note that the Jacobian matrices must be estimated at every prediction step of the Kalman filter [46] that makes the whole process time-consuming. The whole estimation procedure of EKF2 is shown in Fig. 2.

C. UNSCENTED KALMAN FILTER

The requirement of high computation capacity of linearization was a motivation of researchers to propose a new type of nonlinear Kalman filter, which is called Unscented Kalman filter (UKF) [53]–[55]. In this method, the Kalman gain is calculated without linearization of the nonlinear equations. An unscented Transformation (UT) is used instead. A bounded number of sigma points and weights form the Unscented Transformation, by which the Kalman gain is estimated in UKF. A pre-defined number of sigma points are collected deterministically in UT, which exactly obtain the desired mean and covariance of the main distribution (x). Following the spread of the sigma points into the nonlinear function, it is possible to determine the moments (mean and covariance) of the transformed variable [46]. This method,

just like other methods based on the Kalman filter, includes prediction and updating steps. Prediction step includes:

- 1) CREATE $2n + 1$ SIGMA POINTS SELECTED BY THE ALGORITHM

The first sigma point ($i = 0$) is:

$$X_{k-1}^{(0)} = m_{k-1} \quad (21)$$

The next n sigma points ($i = 1, \dots, n$) are:

$$X_{k-1}^{(i)} = m_{k-1} + \sqrt{n + \lambda} \cdot [\sqrt{P_{k-1}}] \quad (22)$$

Finally the second n sigma points ($i = n + 1, \dots, 2n$) are:

$$X_{k-1}^{(i)} = m_{k-1} - \sqrt{n + \lambda} \cdot [\sqrt{P_{k-1}}] \quad (23)$$

where λ is scaling parameter and n is dimension of system.

- 2) SPREAD OF THE $2n + 1$ SIGMA POINTS INTO NONLINEAR DYNAMIC MODEL (AS A BLACK BOX)

$$\hat{X}^{(i)} = f(X_{k-1}^{(i)}) \quad i = 0, \dots, 2n \quad (24)$$

- 3) THE PREDICTED MOMENTS ARE GIVEN BY

The mean value of estimate is predicted as:

$$m^- = \sum_{i=0}^{i=2n} W_i^{(m)} \cdot \hat{X}^{(i)} \quad (25)$$

where $W^{(m)}$ is weighting parameters for mean value calculation and $2n + 1$ weighting parameters are calculated as:

$$W_0^{(m)} = \lambda / (n + \lambda) \quad (26)$$

$$W_i^{(m)} = \lambda / (2 \cdot (n + \lambda)) \quad i = 1, \dots, 2n \quad (27)$$

The covariance of estimate is predicted as:

$$P^- = \sum_{i=0}^{i=2n} W_i^{(c)} \cdot (\hat{X}^{(i)} - m^-) \cdot (\hat{X}^{(i)} - m^-)^T + Q_{k-1} \quad (28)$$

where weighting parameters $W^{(c)}$ for covariance calculation are obtained as:

$$W_0^{(c)} = \lambda / (n + \lambda) + (1 - \alpha^2 + \beta) \quad (29)$$

$$W_i^{(c)} = \lambda / (2 \cdot (n + \lambda)) \quad i = 1, \dots, 2n \quad (30)$$

The predicted mean value and covariance are used in the updating step of UKF to form new set of sigma points and the whole procedure of updating is done in the next three steps (4-6).

- 4) CREATE THE NEW NUMBER OF SIGMA POINTS AS

$$\begin{cases} X^{-(0)} = m^- \\ X^{-(i)} = m^- + \sqrt{n + \lambda} \cdot [\sqrt{P^-}] & i = 1, \dots, n \\ X^{-(i)} = m^- - \sqrt{n + \lambda} \cdot [\sqrt{P^-}] & i = n + 1, \dots, 2n \end{cases} \quad (31)$$

5) SPREAD OF THE SIGMA POINTS INTO NON-LINEAR MEASUREMENT MODEL

$$\hat{y}^{(i)} = h(X^{-(i)}) \quad i = 0, \dots, 2n \quad (32)$$

6) UPDATE THE PREDICTION AND SO THE ESTIMATE IS CALCULATE AT TIME STEP $k + 1$ AS

The updated mean value is:

$$m = m^- + K.(y - \mu) \quad (33)$$

The updated covariance is:

$$P = P^- - K.S.K^T \quad (34)$$

The UKF's gain is:

$$K = C/S \quad (35)$$

The quantities μ , S and C are:

$$\mu = \sum_{i=0}^{i=2n} W_i^{(m)} . \hat{y}^{(i)} \quad (36)$$

$$S = \sum_{i=0}^{i=2n} W_i^{(c)} . (\hat{y}^{(i)} - \mu) . (\hat{y}^{(i)} - \mu)^T + R_k \quad (37)$$

$$C = \sum_{i=0}^{i=2n} W_i^{(c)} . (X^{-(i)} - m^-) . (\hat{\mu}^{(i)} - \mu)^T \quad (38)$$

The whole estimation procedure of UKF is shown in Fig. 3.

D. GAUSS HERMITE KALMAN FILTER

State estimation of a stochastic nonlinear system polluted by noise is characterized in the nonlinear filtering problem. This section aims to examine real-time and appropriate filters for nonlinear filtering problems with Gaussian distributions. The methodical formulation of Gaussian filters is developed in this section. The optimal filter used in this section is based on the Bayesian equation as a recursive numerical integration method. The recursive characteristic ends in the removal of calculation of the Jacobian matrix, which was essential in EKF [56]. The Gauss-Hermite algorithm for filtering is based on the Gauss-Hermite quadrature rule. According to the quadrature rule, a Gaussian density with zero average is considered for the weight function. Analytically, it isn't easy to determine quadrature weights and points for a nonlinear problem. Consequently, a number of proper points are collected as quadratic points. Then, the weights are calculated by estimating the mean and covariance of the integral of quadrature points [57].

Desired moments of the primary distribution of x are obtained precisely by estimating the integrals in the prediction step as follows:

$$m^- = \int f(x_{k-1}) . N(x_{k-1} | m_{k-1}, P_{k-1}) dx_{k-1} \quad (39)$$

$$P^- = Q_{k-1} + \int E . E^T . N(x_{k-1} | m_{k-1}, P_{k-1}) dx_{k-1} \quad (40)$$

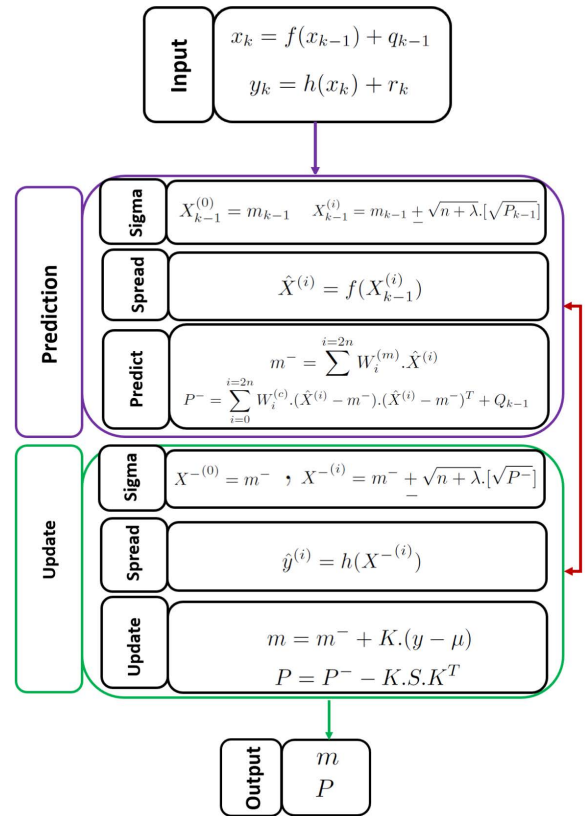


FIGURE 3. Flowchart of UKF.

where $E = f(x_{k-1}) - m_k^-$. In update step the integrals as:

$$m = m^- + K.(y - \mu) \quad (41)$$

$$P = P^- - K.S.K^T \quad (42)$$

where different quantities in (41) and (42) are obtained as:

$$\begin{cases} \mu = \int h(x_k) N(x_k | m^-, P^-) dx_k \\ E = h(x_k) - \mu \\ S = \int E . E^T . N(x_k | m^-, P^-) dx_k + R_k \\ C = \int (x_k - m^-) (h(x_k) - \mu)^T . N(x_k | m^-, P^-) dx_k \\ K = C/S \end{cases} \quad (43)$$

It is possible to solve the integrals in (39) by an analytical integration method or a numerical integration method. However, there is no general and absolute solution for these integrals, so approximate methods must be used to solve them. Gauss-Hermite is one of the approximate methods which is used in this section. A quadrature algorithm based on orthogonal polynomials is Gauss-Hermite integration method used in this section [58]. A weighted sum estimate approach for determining the result of integrals, which is called the Gauss-Hermite rule, is as follows:

$$\int_{R^n} f(X) . e^{-X^T . X} dX \approx \sum_{i=1}^m \omega_i f(X_i) \quad (44)$$

The GHKF algorithm (degree p) also includes two steps; prediction and updating which its prediction step includes following steps:

1) BASED ON THE GAUSS HERMITE THEORY, THE QUADRATURE POINTS ARE DETERMINED TO BE THE ROOTS OF HERMITE POLYNOMIAL WITH THE ORDER p AS FOLLOWS [32]

$$H_p(x) \xrightarrow{\text{roots}} x_i, \quad i = 1, \dots, p \quad (45)$$

2) CALCULATE THE ASSOCIATED WEIGHTS AS

$$\omega_i = \frac{2^{p-1} \cdot p!}{p^2 \cdot [H_{p-1}(x_i)]^2} \quad (46)$$

3) APPLY THE PRODUCT RULE TO DEVELOP THE PREVIOUS POINTS TO AN N-dimeNsioNal LATTICE OF POINTS

$$x_i, i = 1, \dots, p \xrightarrow{\text{n-dimension}} \xi_i, i = 1, \dots, p^n \quad (47)$$

4) CONSIDER THE FOLLOWING POINT AS SIGMA POINTS

$$X_{k-1}^{(i)} = m_{k-1} + \sqrt{P_{k-1}} \cdot \xi_i \quad (48)$$

5) EACH SIGMA POINT IS PASSED INTO THE PROCESS MODEL TO GENERATE A NUMBER OF TRANSFORMED SAMPLES AS

$$\hat{X}^{(i)} = f(X_{k-1}^{(i)}) \quad (49)$$

6) THE PREDICTED MEAN AND COVARIANCE ARE CALCULATED AS

$$m^- = \sum_{i=1}^{p^n} \omega_i \cdot \hat{X}^{(i)} \quad (50)$$

$$P^- = \sum_{i=1}^{p^n} \omega_i \cdot (\hat{X}^{(i)} - m^-) \cdot (\hat{X}^{(i)} - m^-)^T + Q_{k-1} \quad (51)$$

And updating step includes following steps:

7) REPEAT STEP 1-3 OF PREDICTION PART TO GET POINTS AND THEIR WEIGHTS

8) CREATE THE SIGMA POINTS AS

$$X^{- (i)} = m^- + \sqrt{P^-} \cdot \xi_i \quad (52)$$

9) BY APPLYING THE NON-LINEAR MEASUREMENT FUNCTION TO SIGMA POINTS WE HAVE

$$\hat{y}^{(i)} = h(X^{- (i)}) \quad (53)$$

10) BY MEASURING y_k AS A NEW MEASUREMENT y_k , THE UPDATED MEAN AND COVARIANCE CAN BE CALCULATED AS

$$m = m^- + K \cdot (y - \mu) \quad (54)$$

$$P = P^- - K \cdot S \cdot K^T \quad (55)$$

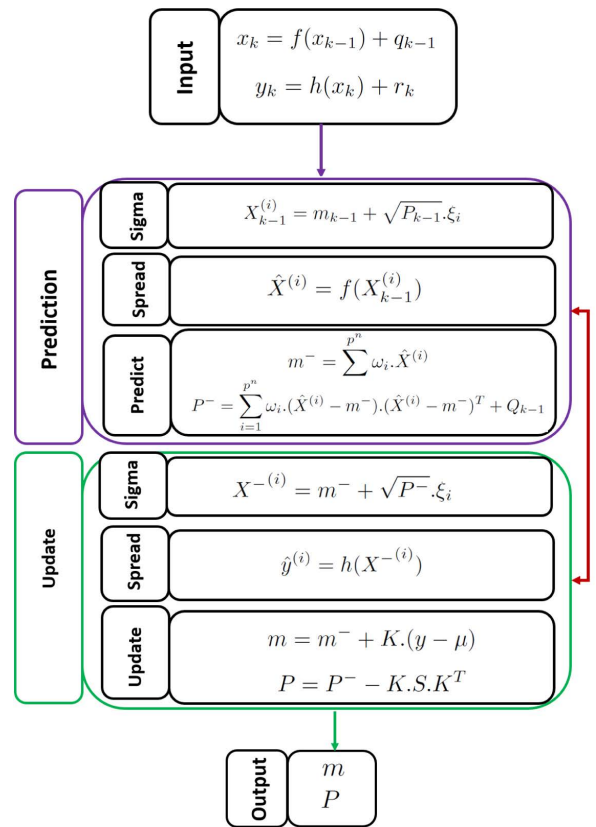


FIGURE 4. Flowchart of GHKF.

where different quantities in (54) and (55) are obtained as:

$$\begin{cases} \mu = \sum_{i=1}^{p^n} \omega_i \cdot \hat{y}^{(i)} \\ S = \sum_{i=1}^{p^n} \omega_i \cdot (\hat{y}^{(i)} - \mu) \cdot (\hat{y}^{(i)} - \mu)^T + R_k \\ C = \sum_{i=1}^{p^n} \omega_i \cdot (X^{- (i)} - m^-) \cdot (\hat{y}^{(i)} - \mu)^T \\ K = C/S \end{cases} \quad (56)$$

The whole estimation procedure of GHKF is shown in Fig. 4. Application of the explained filter is challenging due to dimensional problems because the needed quadrature points grow exponentially with an increase in the system's dimension. The problem of dimensionality causes this method to be highly ineffective with multiple dimensions [59]. Therefore next method (Cubature Kalman filter) is presented in this paper.

E. CUBATURE KALMAN FILTER

A simpler process to solve non-linear integral is given by the spherical radial cubature transformation which is proposed first by [47]. Compared to GHKF, the integrals required to be determined are identical, but the numerical integration technique is changed. Cubature Kalman filter (CKF) is used in this section as a nonlinear filter with the ability to handle

a system with high dimensions to estimate the state accurately. The nonlinear filter is originated from the Spherical-Radial Cubature rule and Bayesian theory. Cubature Kalman filter is stable and accurate numerically due to all positive cubature point weights when propagating the states and covariance matrix. It ensures the positive definiteness of the covariance matrix of the filtering process [60], [61]. Moreover, in CKF, unlike the EKF, the Jacobians matrix construction and calculation are eliminated under the state estimation procedure. It will be promising for the state estimation of a nonlinear system [62]. The cubature Kalman filter (CKF) method is described in the following section. Prediction step includes:

1) THE CKF USES 2n SIGMA POINTS

The first n sigma points (i = 1, . . . , n) are obtained by:

$$\delta_i = \sqrt{n}.c_i \tag{57}$$

The second n sigma points (i = n + 1, . . . , 2n) are obtained by:

$$\delta_i = -\sqrt{n}.c_{i-n} \tag{58}$$

where c₁ = [1, 0, 0, . . . , 0]^T, c₂ = [0, 1, 0, . . . , 0]^T, c₃ = [0, 0, 1, . . . , 0]^T and so on. It is worth noting that the Cubature Kalman filter is one kind of filtering algorithm that uses different forms of numerical integration to handle measurement and process nonlinearities. The set of sigma points is representative and represents the nonlinearity of the function and are selected in a reasonable range to increase the accuracy approximation and, finally, estimation process. The sigma points in (57) and (59) are selected based on the Spherical-Radial Cubature rule, which is one by one perpendicular.

2) FORM THE SIGMA POINTS AS

$$X_{k-1}^{(i)} = m_{k-1} + \sqrt{P_{k-1}}.\delta_i \tag{59}$$

3) SPREAD THE SIGMA POINTS INTO THE NONLINEAR DYNAMIC MODEL

$$\hat{X}^{(i)} = f(X_{k-1}^{(i)}) \tag{60}$$

4) THE PREDICTED MEAN AND COVARIANCE ARE CALCULATED AS

$$m^- = \sum_{i=1}^{p^n} \omega_i.\hat{X}^{(i)} \tag{61}$$

$$P^- = \sum_{i=1}^{p^n} \omega_i.(\hat{X}^{(i)} - m^-).(\hat{X}^{(i)} - m^-)^T + Q_{k-1} \tag{62}$$

where w_i = 1/(2.n). And updating step includes:

5) CREATE NEW SIGMA POINTS BASED ON THE PREDICTED MOMENTS AS

$$X^{- (i)} = m^- + \sqrt{P^-}.\delta_i \tag{63}$$

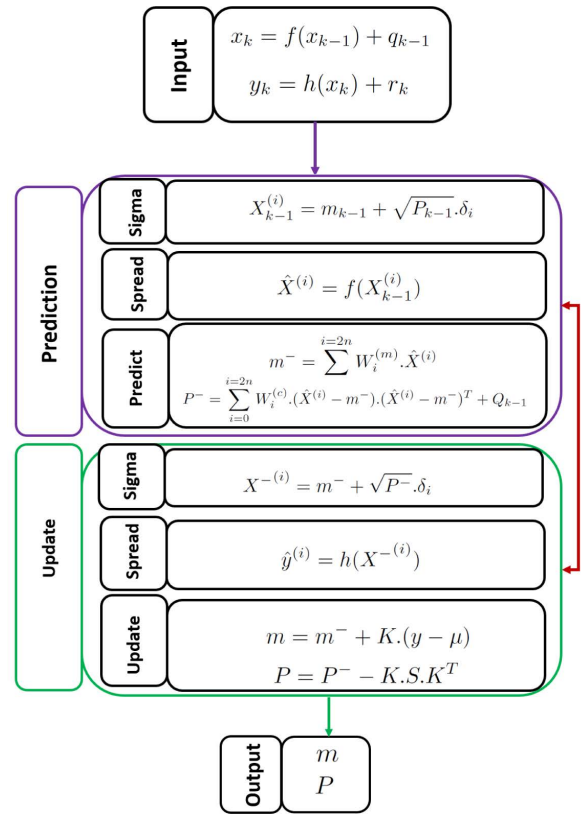


FIGURE 5. Flowchart of CKF.

6) SPREAD THE SIGMA POINTS INTO THE NONLINEAR MEASUREMENT MODEL

$$\hat{y}^{(i)} = h(X^{- (i)}) \tag{64}$$

7) DETERMINE THE POSTERIOR MEAN AND COVARIANCE FROM CURRENT MEASUREMENT AS

$$m = m^- + K.(y - \mu) \tag{65}$$

$$P = P^- - K.S.K^T \tag{66}$$

where

$$\begin{cases} \mu = \sum_{i=1}^{p^n} \omega_i.\hat{y}^{(i)} \\ S = \sum_{i=1}^{p^n} \omega_i.(\hat{y}^{(i)} - \mu).(\hat{y}^{(i)} - \mu)^T + R_k \\ C = \sum_{i=1}^{p^n} \omega_i.(X^{- (i)} - m^-).(\hat{y}^{(i)} - \mu)^T \\ K = C/S \end{cases} \tag{67}$$

The whole estimation procedure of CKF is shown in Fig. 5. Moreover, an integrated figure is shown in Fig. 6, in which the difference between different filters is presented. A single integrated picture compares the nonlinear Kalman filters as an evolution with the core Kalman filter as the center and other variants evolving around it. This would illustrate how each of them is different from the others.

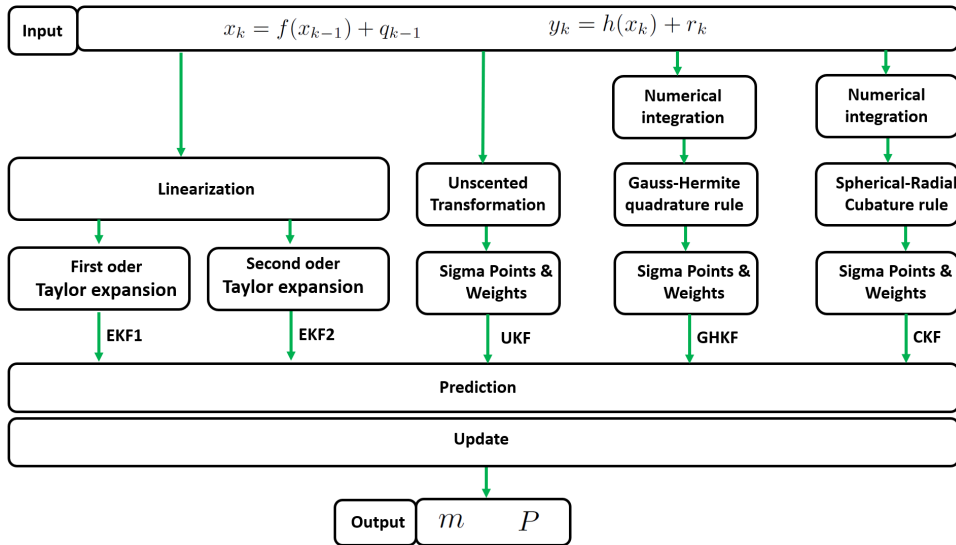


FIGURE 6. Integrated picture showing the comparison of the nonlinear Kalman filters.

III. DYNAMIC PHASOR ESTIMATION

According to the classical definition of the phasor, it is a complex envelope of a sinusoidal function with fixed amplitude, phase, and frequency. However, phasor estimation in a real power system is more challenging, and the parameters change over time. Dynamic phasor is a more accurate notion for phasor estimation during the dynamic condition when the amplitude and phase are not constant values. In this paper, amplitude and phase have been considered time-dependent variables [63] in the definition of the phasor, and tests with the same characteristics are considered for evaluation of the estimation methods. Since the first and second derivatives of phasor are used in the dynamic phasor concept, they can be utilized for further analysis in other fields such as the protection of power systems. Quick detection of power swing in a protection system (distance relay) of a transmission line can be an application of derivatives of the dynamic phasor. Some methods for power swing detection are presented in [64]–[67].

Consider a sinusoidal quantity with variable amplitude and phase as:

$$y(t) = a(t)\sin(\omega_1 t + \phi(t)) \quad (68)$$

where $a(t)$ is amplitude, $\phi(t)$ is phase angle of main signal $y(t)$. ω_1 is the angular frequency of the signal. The dynamic phasor is defined as:

$$p(t) = a(t)e^{j\phi(t)} \quad (69)$$

According to (69), a new concept of the phasor is not a constant complex value. Instead, it is a dynamic complex parameter whose amplitude and phase change during time according to different conditions in the power system. By considering the time-variant characteristic of amplitude and phase of the dynamic phasor, a state-space for nonlinear Kalman filter will be formed in the next section.

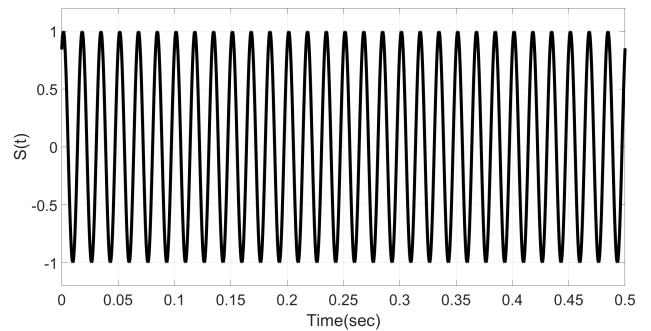


FIGURE 7. Main signal under steady-state conditions.

A. STATE SPACE FOR NONLINEAR KALMAN FILTER

State-space is the heart of any Kalman filter. It actually relates between the system’s dynamics in two consecutive sample times and the state of system and input measurement in the current sample. Based on the presented definition for dynamic phasor and description of non-linear Kalman filter (presented in the previous section), the filters state spaces consist of the amplitude and phase as:

$$\begin{bmatrix} a(k\Delta t) \\ \phi(k\Delta t) \end{bmatrix} = \begin{bmatrix} \Delta t & 0 \\ 0 & \Delta t \end{bmatrix} \begin{bmatrix} a((k-1)\Delta t) \\ \phi((k-1)\Delta t) \end{bmatrix} + q_{k-1} \quad (70)$$

$$y(t) = \begin{bmatrix} 1 \\ 0 \end{bmatrix}^T \begin{bmatrix} a(k\Delta t) \\ \phi(k\Delta t) \end{bmatrix} \sin(\omega t + \begin{bmatrix} 1 \\ 0 \end{bmatrix}^T \begin{bmatrix} a(k\Delta t) \\ \phi(k\Delta t) \end{bmatrix}) + r_k \quad (71)$$

where $\omega = 2\pi f_1$ is fundamental angular frequency. Equations (70) and (71) construct the state space of dynamic phasor estimation. According to these equations, amplitude and phase are considered time-varying parameters. This state space is used by five presented nonlinear Kalman filters, and amplitude and phase of the main signal (dynamic phasor)

are estimated which their results will be shown in the next section.

IV. SIMULATION RESULTS

As explained in the IEEE standard, a specific method for estimation in the phasor measurement unit (PMU) and its behavior is out of the standard's scope. However, some simple tests are proposed in the standard to assess these behaviors. The nonlinear Kalman filters have been developed in the previous sections. This section analyzes the performances for five nonlinear Kalman filters for dynamic phasor estimation by different tests (steady state condition, sinusoidal amplitude and phase, step change of amplitude and phase, off-nominal frequency, fault condition, DC component and harmonic infiltration, simulation time, and noise infiltration). Moreover, the advantage of the nonlinear Kalman filter compared to the linear Kalman filter will be shown in this section. Finally, the performance of the nonlinear Kalman filter is compared with six methods that have already been published in the literature. All simulations are done in a MATLAB environment.

A. STEADY-STATE COMPLIANCE

This section deals with measurement compliance tests and performance limits under steady-state conditions [68], [69]. Steady-state compliance is confirmed by comparing the estimates of synchrophasor under steady-state conditions to the reference values. Consider the test signal

$$S(t) = a_m \sin(\omega t + \phi_m) \tag{72}$$

where $a_m = 1 \text{ p.u}$ is amplitude, $\phi_m = 57^\circ$ is phase angle, $\omega = 2\pi f$ is frequency of signal. The main signal is shown in Fig. 7. The proposed method is applied to the test signal (72) with sampling frequency 3.84 KHz and nominal frequency of 60 Hz . Variance value of process and observation noises are considered 10^{-4} , which matches a signal-to-noise ratio (SNR) of 37 dB , similar to the SNR a 6-bit analog to digital converter. The initial condition of the state is $[0 \ 0]^T$, and its associated covariance matrix is $P = 3I$ (where I is the identity matrix). During the steady-state condition, the amplitude, angle, and frequency are kept constant. Total Vector Error (TVE) accuracy criterion is given by:

$$TVE = \left| \frac{X_r - X_e}{X_r} \right| \tag{73}$$

where X_r is real phasor, and X_e is the estimated phasor.

Five Kalman filters are applied to 1 second of main signal presented in (72). Fig. 8 shows estimated amplitude, estimated angle and accuracy of estimation (TVE) by five nonlinear Kalman filters during steady-state condition as the first test case proposed in the IEEE standard for synchrophasor estimation. According to Fig. 8, all methods meet the accuracy requirement ($TVE < 1\%$) in a steady-state condition.

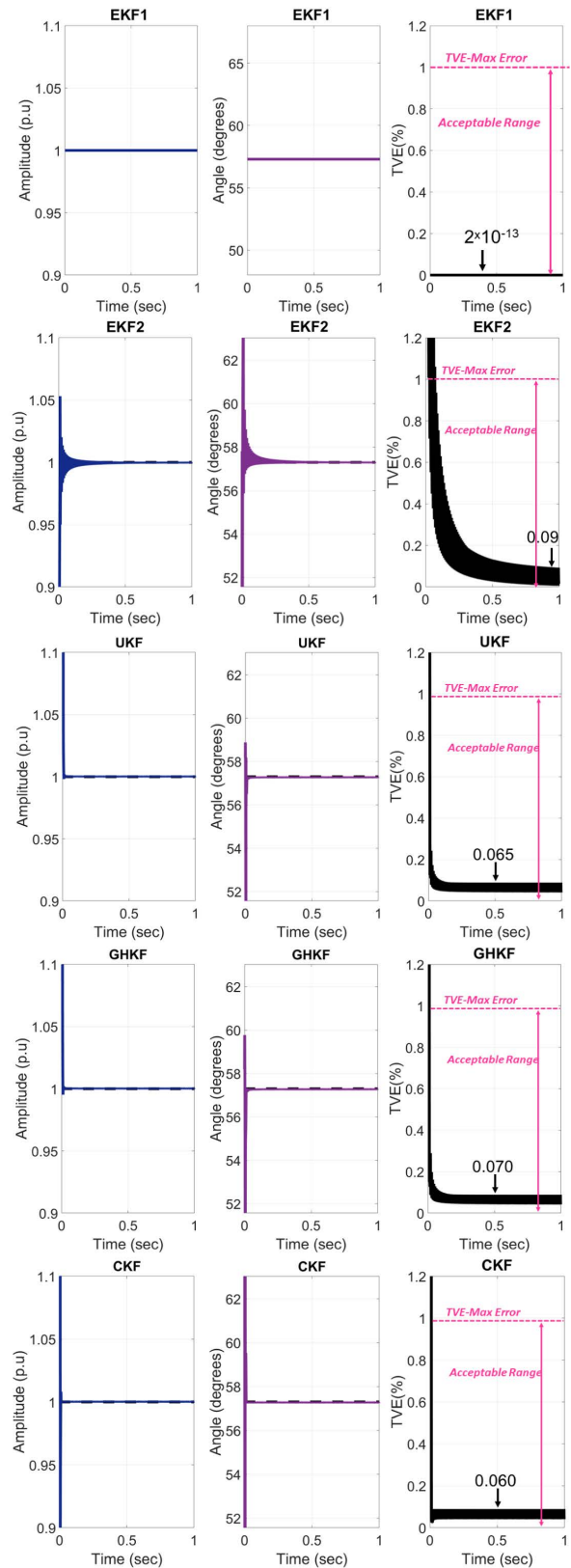


FIGURE 8. Performance of five non-linear Kalman filters under steady-state conditions.

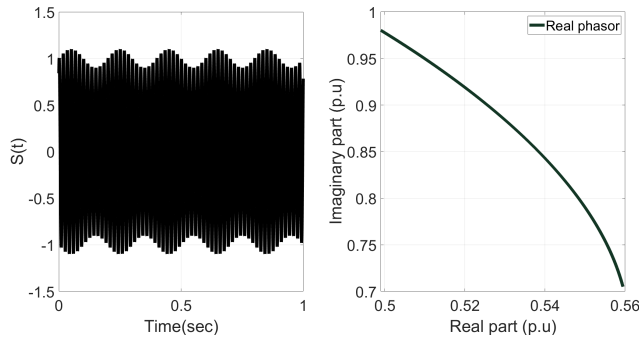


FIGURE 9. Main signal under dynamic condition (modulated amplitude and phase) and the real phasor.

B. DYNAMIC COMPLIANCE MEASUREMENT BANDWIDTH

In this section, the performance of five nonlinear Kalman filters are compared when the amplitude and phase of the main signal change sinusoidally. Consider test case (74) as follows:

$$S(t) = a(t) \sin(\omega + \phi(t)) \tag{74}$$

where

$$\begin{cases} a(t) = a_m + (k_x \sin(\omega_{osc}t)) \\ \phi(t) = \phi_m + (k_a \sin(\omega_{osc}t)) \\ a_m = 1; \phi_m = 57^\circ, k_x = 0.1, k_a = 0.1, \omega_{osc} = 10\pi \end{cases}$$

where $a(t)$ is the modulated amplitude of, ω is the fundamental angular frequency, $\omega_{osc} = 10\pi$ is the modulation frequency (5Hz oscillation is proposed in the IEEE standard as a fast modulating frequency), $k_a = 0.1$ and $k_x = 0.1$ are the amplitude and phase angle modulation factors. sampling frequency 3.84 KHz and nominal frequency of 60Hz. Process and observation noises are considered 10^{-2} and 10^{-4} respectively. The initial condition of the state is $[0 \ 0]^T$, and its associated covariance matrix is $P = 3I$. Fig. 9 shows the main signal presented in (74) and its real phasor. This test case validates application of the dynamic phasor concept since the phasor is changing with time. Five filters are applied to (74) and the results (estimated phasor and TVE) are shown in Fig. 10. The maximum allowable value of TVE (3%) during dynamic condition (modulated amplitude and phase), proposed by IEEE standard is also specified in Fig. 10. Fig. 10 shows that the standard’s requirement of TVE for both P-class and M-class PMU is met in all five nonlinear Kalman filters.

C. DYNAMIC COMPLIANCE (PERFORMANCE UNDER STEP CHANGES IN PHASE AND MAGNITUDE)

To evaluate an estimation method’s performance under transition between two steady-state conditions, step-change in amplitude and phase are specified in the standard. In this section, the behavior of five nonlinear Kalman filters is examined when the amplitude and phase of the main signal change step-like.

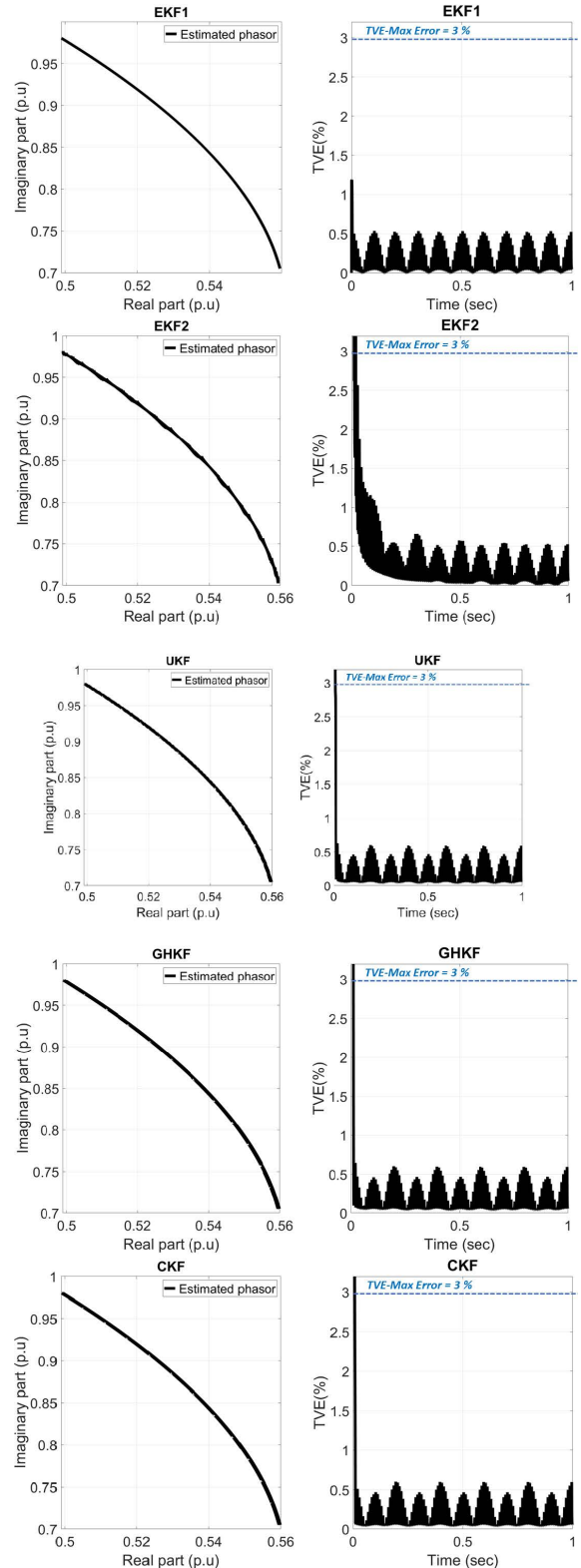


FIGURE 10. Performance of five non-linear Kalman filters under dynamic conditions (modulated amplitude and phase).

1) AMPLITUDE STEP TEST

Consider the test waveform presented in (75) shown in Fig. 11. It shows 10% magnitude step at $t = 1sec$.

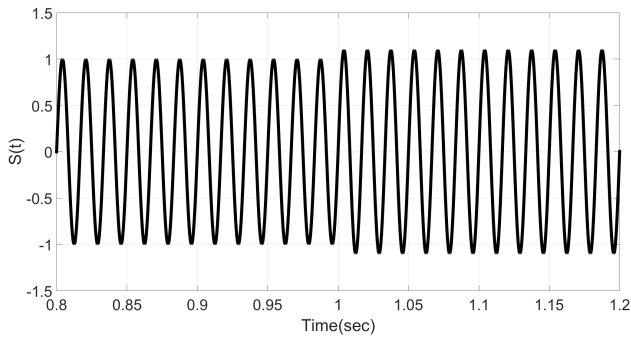


FIGURE 11. Main signal under step change of amplitude.

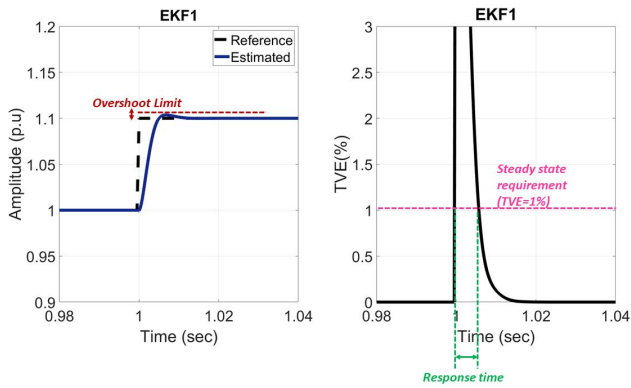


FIGURE 12. Estimated amplitude and TVE by EKF1 under step change of amplitude.

Sampling time, process and observation noises, and the initial condition of state and its associated covariance matrix are similar to section IV.A. Simulation results of the test case for five filters are obtained but just the results (estimated amplitude and TVE) of EKF1 are shown in Fig. 12. According to Fig. 12, the reference amplitude is tracked accurately. According to the standard and Fig. 12, the response time (the time when TVE reached less than $TVE = 1\%$ after step change), and maximum value of overshoot are calculated and tabulated in Table 1. The response times and overshoots of the rest four filters (EKF2, UKF, GHKF and CKF) are tabulated in Table 1, section “amplitude”. According to Table 1, all filters meets the overshoot requirement for both P-class (5%) and M-class PMU (10%). Moreover, all filters meets the requirement of response time for P class ($1.7/f_0 = 0.0283s$) and M class of a PMU.

$$\begin{cases} S(t) = a_m \sin(\omega t + \phi_m) \\ a_m = 1, \quad \phi_m = 0 & 0 < t < 1sec \\ a_m = 1.1, \quad \phi_m = 0 & t > 1sec \end{cases}$$

2) PHASE STEP TEST

Consider the test waveform presented in (76), which shows 10^0 phase angle step at $t = 1sec$. Sampling time, process and observation noises, and the initial condition of state and its

TABLE 1. Overshoots and response times of different filters during step changes (amplitude and phase).

Test (step in)	Filter	Overshoot (%)	Response time (ms)
Amplitude	EKF1	4	5.6
	EKF2	3.2	5.6
	UKF	4.4	5.7
	GHKF	4.5	5.7
	CKF	4.5	5.6
Phase	EKF1	0.85	7.5
	EKF2	0.84	7.6
	UKF	0.75	7.4
	GHKF	0.74	7.4
	CKF	0.75	7.4

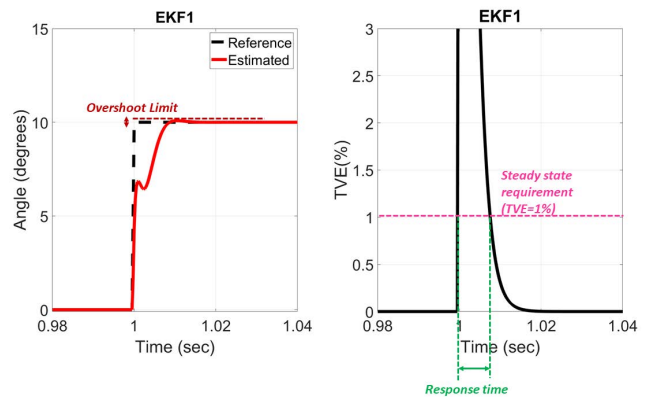


FIGURE 13. Estimated phase and TVE by EKF1 under step change of phase angle.

associated covariance matrix are similar to section IV.A.

$$\begin{cases} S(t) = a_m \sin(\omega t + \phi_m) \\ a_m = 1, \quad \phi_m = 0 & 0 < t < 1sec \\ a_m = 1, \quad \phi_m = 10^0 & t > 1sec \end{cases} \quad (75)$$

Simulation results (estimated amplitude and TVE) of EKF1 are shown in Fig. 13. According to Fig. 13, EKF1 could follow the variation of reference value of phase angle accurately and based on the IEEE standard, the response time due to step change is 7.5 ms, which is much smaller than the requirement for both classes of PMUs. Moreover, overshoot of estimated angle is 0.85%, which is smaller than the requirement 5%. Simulation results of all filters are tabulated in Table 1, section “phase”. According to Table 1, all filters meets the requirements of standard for both P-class and M-class of PMUs.

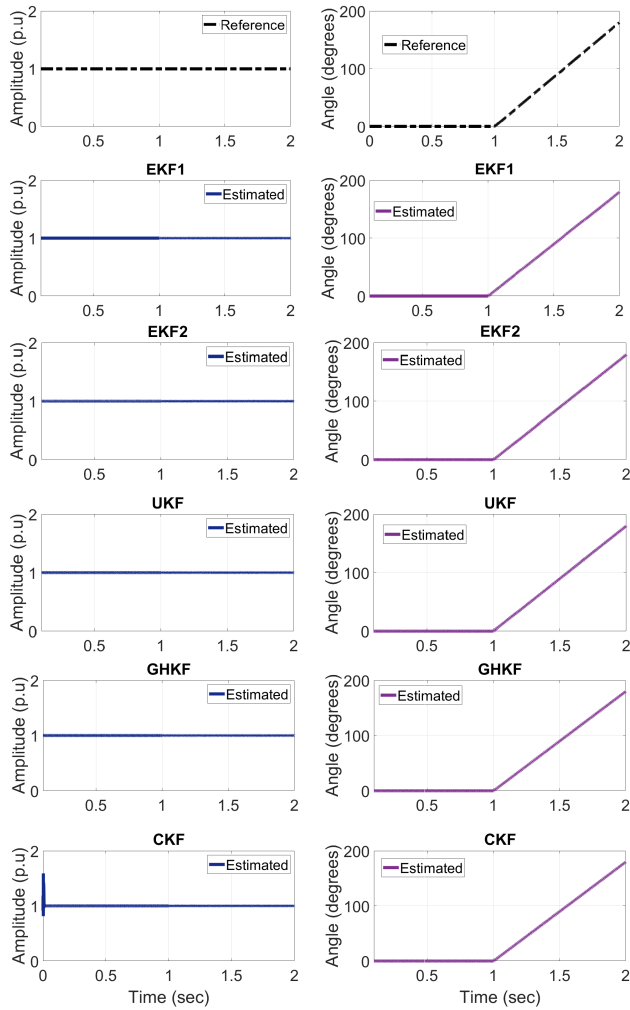


FIGURE 14. Amplitude and phase estimation under off-nominal frequency test case.

3) OFF-NOMINAL FREQUENCY

The next test case is a 0.5 Hz frequency deviation from fundamental frequency $f_0 = 60\text{Hz}$. The test waveform is presented in (77).

$$\begin{cases} S(t) = \sin(2.\pi.f_0.t) & 0 < t < 1 \\ S(t) = \sin(2.\pi.(f_1 + 0.5).t) & t > 1 \end{cases} \quad (76)$$

Sampling time, process and observation noises, and the initial condition of state and its associated covariance matrix are similar to section IV.A. Fig. 14 shows amplitude and phase estimates when subjected to off-nominal frequency. According to Fig. 14, amplitude and phase are estimated accurately by all filters.

D. TYPICAL CASE IN A POWER SYSTEM

In this section a more common waveform in a power system is evaluated by the five filters. First, the system is under steady state condition. Then suddenly a fault accrues and removed after a few milli-seconds. Removing fault creates DC component and power swing in the measured voltage

TABLE 2. Contingencies generation.

Section	Type	Explanation
IV.D	Three-phase fault+	Solid fault at $t=0.1 (t_1)$
	Frequency components (DC+300 Hz)	Removed at 0.2 s (t_2)
IV.G.1	Three-phase fault	Low impedance ($Z_f = 0$) $t_1 = 1\text{ s} , t_2 = 1.1\text{ s}$
IV.G.2	Three-phase fault	High impedance ($Z_f = 10$) $t_1 = 1\text{ s} , t_2 = 1.1\text{ s}$
IV.G.3	Load level change	Initial value= $S=320+j153$ Final value=0, $t_1 = 1\text{ s}$

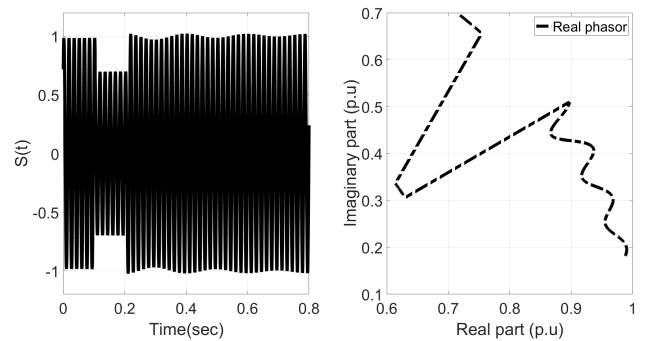


FIGURE 15. Main signal and real phasor in case IV.C.

and current. Additionally, in reality, the signals measured in a power system may contain harmonics. The same scenario is presented [22], which is re-simulated in MATLAB. The waveform is shown in Fig. 15, which shows behaviour of power system in different time periods and consists of a fundamental frequency component (60Hz), fifth harmonic (300Hz) component, DC component and power swing. Parameters involved in the contingency of this section are summarized in Table 2, second row.

There are 64 samples in one fundamental cycle. Sampling time, process and observation noises, and the initial condition of state and its associated covariance matrix for non-linear Kalman filters are similar to section IV.A. Simulation results (estimated phasor and TVE) obtained by five non-linear Kalman filters are shown in Fig. 16. All five filters track variation of phasor during steady state and dynamic conditions and accuracy of estimation (TVE) is less than the requirement for PMU. It is worth to note that TVE exceed the limit (1%) just at fault incident and fault removing that is allowable as presented in standard.

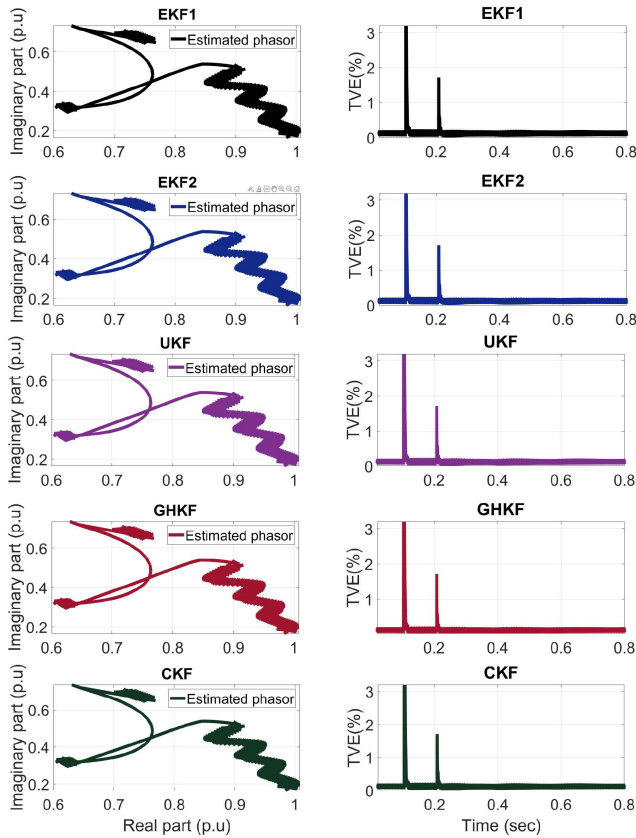


FIGURE 16. Estimated phasor and corresponding TVE for five infiltration test case IV.C.

E. SIMULATION TIME

Simulation time is a key index in online signal processing applications, so this index is examined in this section. The computation time of five nonlinear Kalman filters is examined in this section when the sample number increases from 8 to 1024 samples per cycle. Process and observation noises, the initial state condition, and its associated covariance matrix are considered similar to section IV.A. Simulation result of this test is shown in Fig. 17. According to Fig. 17, the calculation time of all methods shows an upward trend when the sample number increases, and it can be seen that GHKF is the most time-consuming method. The simulation result of another test is also shown in Fig. 18. In this test, simulation time versus state number is examined. According to Fig. 18, increase in state number causes an increase in simulation time, and similar to the previous test, GHKF is the most time-demanding method.

F. NOISE INFILTRATION

Noise phenomena are always present as an unwanted parameter which can reduce the quality of parameter estimation methods. It is helpful to examine the estimation error while the noise level varies. Fig. 19 shows TVE as a function of noise level (SNR) for five filters when subjected to Gaussian

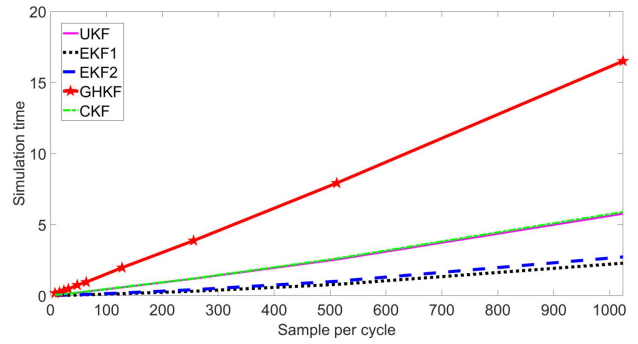


FIGURE 17. Computation time comparison.

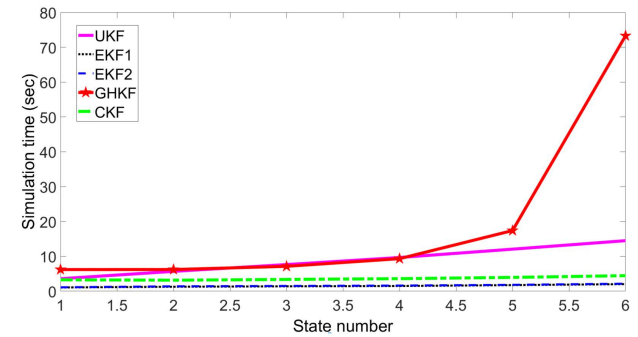


FIGURE 18. Simulation time comparison versus dimension number.

and Non-Gaussian noise. According to Fig. 19, As the SNR decrease, higher TVE are obtained by all methods. So there is an upward trend when the noise level increases. Different filters have different performances under Gaussian and Non-Gaussian noises. Under Gaussian noise, the filters exceed the limit of TVE (1%) when SNR is less than 40 dB but this critical point is 35 dB under Non-Gaussian noise. Moreover, EKF1 shows the most accurate performance in low level noise in both types of noises.

To enrich the noise section, performance of five non-linear Kalman filters are also evaluated by colored noise (Pink, White, Brown, Blue and Purple). The colored noise is a signal with a power spectral density of $1/|f|^\alpha$ over its entire frequency range. The inverse power spectral density component, α , can be any value in the interval $[-2, 2]$. Pink noise is equivalent to setting Power of inverse frequency to 1, white is to zero, brown is to +2, blue is to -1 and purple is to -2. Performance of five filters are examined in different type of colored noises and the results are shown in Fig. 20. Downward trends from low SNR to high SNR are evident in Fig. 20, which demonstrate higher estimation accuracy in lower noise infiltration. However the filters have different critical points in different color of noise. In pink noise, the critical point is approximately 38 dB for all filters, which shows that the filters can not meet the requirement of IEEE standard if SNR would be less than 38 dB. The critical point in white noise is 35 dB, 40 dB in Brown noise, 34 dB in Blue noise and

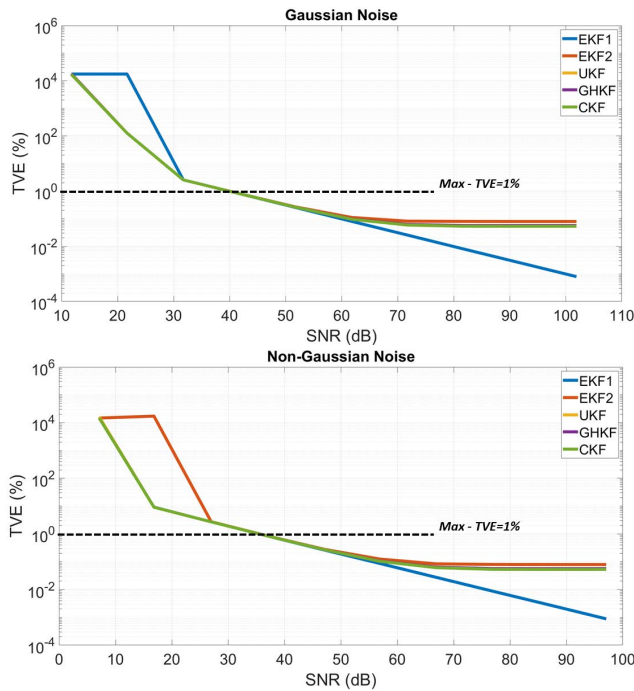


FIGURE 19. Impact of Gaussian and Non-Gaussian noise on accuracy (TVE) of estimates by five filters.

33 dB in Purple noise. The simulation results presented in Fig. 20 show that the filters show a better performance under Purple noise. Additionally, EKF1 is the most accurate type of filter in low level of noise.

G. PERFORMANCE OF NONLINEAR KALMAN FILTERS IN IEEE 39-BUS SYSTEM SIMULATED IN POWERFACTORY

The IEEE 39-Bus power system shown in Fig. 21 is a standard for dynamic performance analysis. A dynamic model of the whole system is simulated in GIGSILENT. In this system, a distance relay is installed in the transmission line on Bus 14. A distance relay is performed by measuring the impedance calculated by the voltage and current phasors. In this section, the measured current by a distance relay is applied to the five nonlinear Kalman filters, and the results will be presented. This section evaluates the nonlinear Kalman filters with measured current by the distance relay (current in transmission line 14-04). The power system is simulated in different contingencies with EMT simulation. Parameters involved in the contingency of this section are summarized in Table 2. Since the real phasor of signal (used in TVE index) is not available in a real power system, the index of phasor estimation error (PEE) is used to evaluate the accuracy of EMD-Prony. PEE is:

$$PEE(n) = |s(n) - \hat{s}(n)|, \quad \hat{s}(n) = |\hat{p}(n)|\cos(n\theta + \hat{\angle}(n)) \tag{77}$$

where n is sample number, $\theta = 2\pi/N$, $s(n)$ is measured signal and $\hat{s}(n)$ is recomputed sample based on estimated phasor.

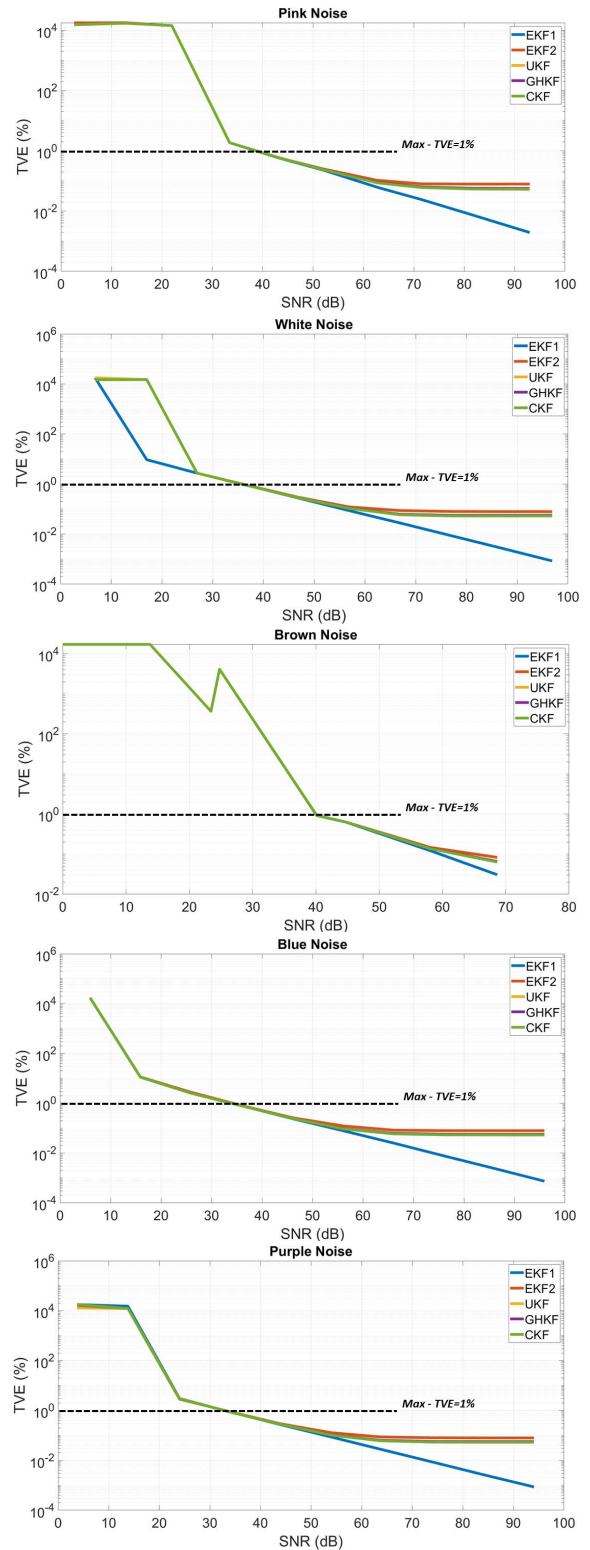


FIGURE 20. Impact of colored noise (Pink, White, Brown, Blue and Purple) on accuracy (TVE) of estimates by five filters.

1) CASE 1: LOW IMPEDANCE FAULT

A three-phase fault with a low impedance ($Z_f = 0$) is applied to Bus 16 at $t = 1\text{sec}$, and the fault is removed after 0.1sec . The system is simulated for 2 sec, and the measured current

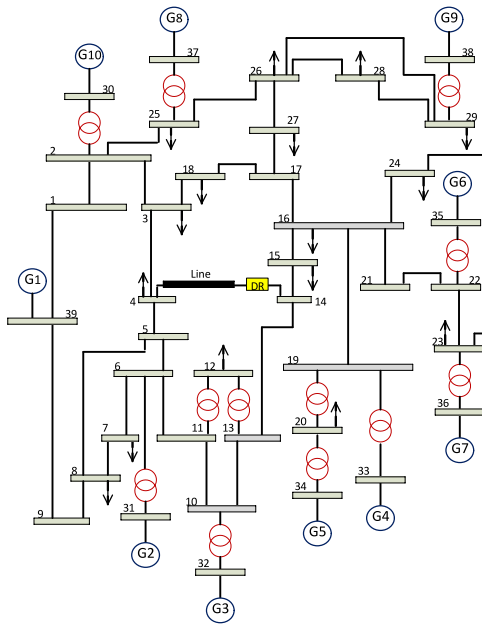


FIGURE 21. IEEE 39-Bus power system.

is shown in Fig. 22 (a). The five nonlinear Kalman filters are applied to the measured current. Fundamental frequency component (60Hz). There are 64 samples in one fundamental cycle. Sampling time, process and observation noises, and the initial condition of state and its associated covariance matrix for non-linear Kalman filters are similar to section IV.A. The PEE of filters are tabulated in Table 3 (second column). It is worth noting that the maximum value of PEE during steady-state and dynamic conditions is presented in Table 3, and the sudden change of PEE during transient conditions is neglected. For page limit, only estimated amplitude and PEE of CKF are shown in Figure 23, the first column. Figure 23 and Table 3 show that the filters can appropriately track amplitude and phase and give the correct phasor for monitoring and protection systems.

2) CASE 2: HIGH IMPEDANCE FAULT

The second case is related to the evaluation of non-linear Kalman filters when there is a high impedance fault in the power system. A high impedance fault ($Z_f = 10\omega$) occurred on Bus 16 at $t = 1sec$ and is removed at 1.1 sec. The measured current by the distance relay is shown in Fig. 22(b). Performance of five non-linear Kalman filters in the estimation of phasor of current are shown in Table 3, third column. Moreover, CKF's performance (estimated amplitude and PEE) are shown in Fig. 23, second column.

3) CASE 3: LOAD CHANGE

Load level change is the third contingency considered in this section. The level of load on Bus 15 suddenly drops to zero at $t = 1sec$. Measured current by the distance relay is shown

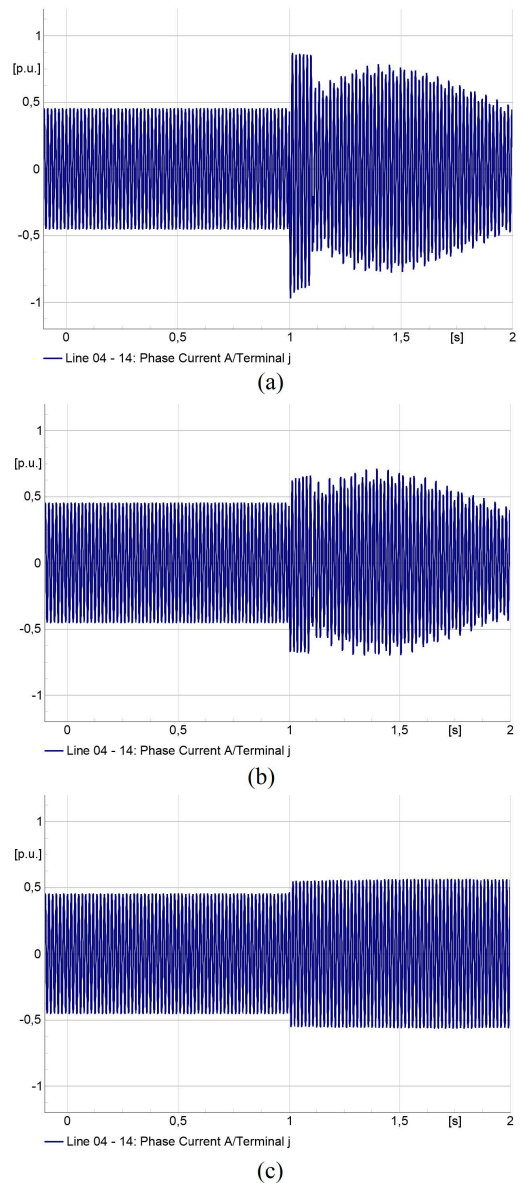


FIGURE 22. Measured current in Line 04-14 in IEEE power system, (a) is for case 1, (b) for case 2, and (c) for case 3.

in Fig. 22 (c). The current is evaluated by five filters, and the corresponding and PEE are presented in Table 3, fourth column. Estimated amplitude and PEE of CKF are also shown in Figure 23, third column.

H. COMPARISON WITH OTHER DYNAMIC PHASOR METHODS

In order to compare the presented methods in this paper with other presented methods in the literature, six different methods which are already published in the literature are programmed in MATLAB and used in this section. The six methods are based on two general observers, so the first three of them are least square-based methods, and the others are the Kalman filter-based methods. These six methods are:

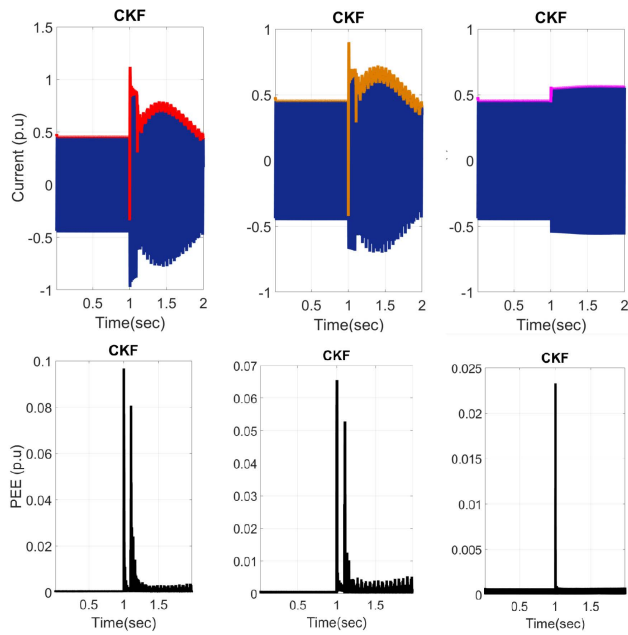


FIGURE 23. CKF's performance; Estimated amplitude and PEE corresponding to three contingencies in section IV.G, the first column is for case 1, second column for case 2, and the third column for case 3.

TABLE 3. Simulation result of section IV.G; maximum PEE (p.u) of different filters.

Method	Case 1	Case 2	Case 3
EKF1	3×10^{-3}	4×10^{-3}	8×10^{-5}
EKF2	3.8×10^{-3}	2.9×10^{-3}	5×10^{-4}
UKF	3.5×10^{-3}	4.5×10^{-3}	7.4×10^{-4}
GHKF	3.7×10^{-3}	5×10^{-3}	7.5×10^{-4}
CKF	3.7×10^{-3}	5×10^{-3}	7.2×10^{-5}

- Traditional: This method employs a Taylor expansion of dynamic phasor with the order of zero and least square observer to estimate phasor [22].
- Fourier-Taylor: This method is based on a Taylor expansion of dynamic phasor with the order two and a least square observer to approximate the dynamic phasor, which is proposed in [22].
- Shank: This method is based on consecutive delays of unit response (digital filter theory) and least square observer to estimate dynamic phasor, which is proposed in [70].
- Kalman-Taylor: this method is based on second-order Taylor expansion of dynamic phasor and a linear Kalman filter to estimate dynamic phasor, which is proposed in [71].
- Fourier-Kalman-Taylor : The main idea of this method is based on introducing augmented state space in linear

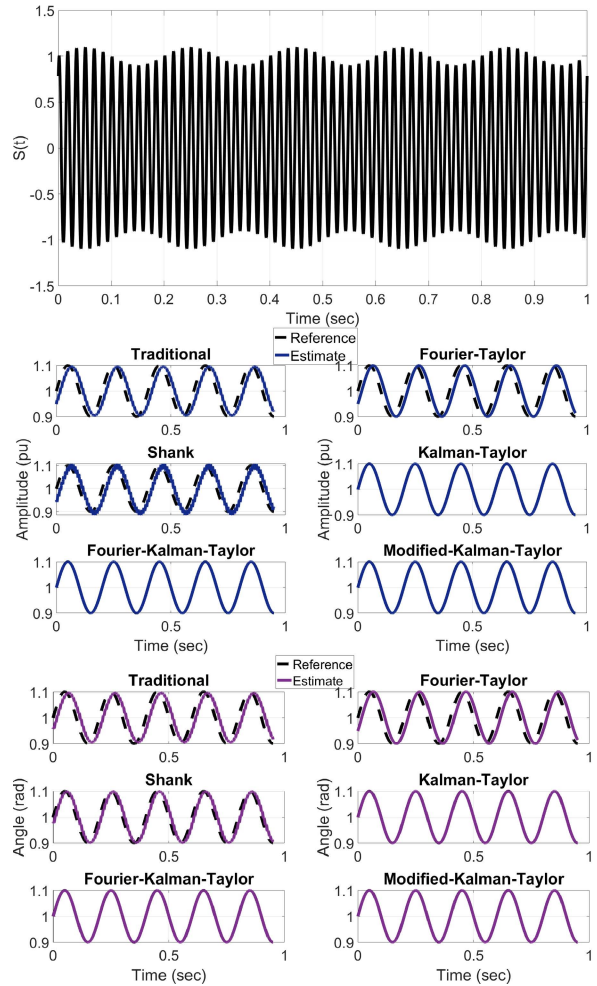


FIGURE 24. Simulation results of section IV.G (main signal(S(t)), amplitude estimation and angle estimation).

Kalman filter which can overcome harmonic infiltration problem [21].

- Modified-Kalman-Taylor: The main contribution of this method is to modify the modeling process of state space of linear Kalman filter to decrease error bound [72].
First, the oscillating test signal presented in (74) is employed to analyze the performance of the six mentioned methods for the estimation of amplitude and phase. Sampling time, process and observation noises, and the initial condition of state and its associated covariance matrix are similar to section IV.A. Except for “Traditional” method that is modeled by a zeroth-order Taylor, all other methods are modeled by a second-order Taylor. Estimated amplitude and estimated phase based on dynamic phasor concept are shown in Fig. 24. Reference signals are shown in dashed lines, and solid lines show the estimated signals. According to Figs. 24, the created delay is the main difference between the results of Kalman-based methods (Methods “Kalman-Taylor”, “Fourier-Kalman-Taylor”, and “Modified-Kalman-Taylor”) and least square-based methods (Methods “Traditional”, “Fourier-Taylor”, and “Shank”).

TABLE 4. Comparison of different methods (accuracy and speed).

Method	TVE%	Simulation time (sec)
EKF1	0.1303	0.5491
EKF2	0.1028	0.5767
UKF	0.1107	0.5913
GHKF	0.1107	1.0288
CKF	0.1101	0.6148
Traditional	0.1729	2.8197
Fourier-Taylor	0.0901	2.8962
Shank	0.1256	2.2174
Kalman-Taylor	0.0980	0.7012
Fourier-Kalman-Taylor	0.0990	4.5360
Modified-Kalman-Taylor	0.0910	0.7519

The created delay is caused by the data window utilized in the least square-based methods. Kalman filter-based methods can give instantaneous estimations (zero-delay), which is a favorable outcome in the field of wide-area monitoring, protection, and control. A required characteristic of these kinds of applications is the synchrony which is granted by Kalman-based methods. As the second result of this section, dynamic phasor concept (Methods “Fourier-Taylor”, “Shank”, “Kalman-Taylor”, “Fourier-Kalman-Taylor”, and “Modified-Kalman-Taylor”) compared to first method (Method “Traditional”) is more flexible in oscillating conditions. In Method “Traditional”, a slight distortion appears at estimated amplitude (Fig. 24) while this distortion disappears in other methods. This improvement is caused due to relaxing amplitude and phase in dynamic phasor model. TVEs and simulation times of different methods are tabulated in Table 4.

V. CONCLUSION

Generally, the Kalman filter calculates the two moments of the distribution (mean and covariance) recursively, resulting from its distinctive predictor-corrector structure. One of the applications of the Kalman filter can be an estimation of the dynamic phasor. The difficulty facing calculating dynamic phasor by Kalman filter is its nonlinear function. Therefore, employing of nonlinear Kalman filter is proposed in this paper. Implementations of five different nonlinear Kalman filters for estimating dynamic phasor are developed and demonstrated in this paper. The appropriate performance of these methods can be figured out from simulation results which demonstrate the accurate tracking of amplitude and phase in all methods. Moreover, the performance of nonlinear Kalman filters is compared with methods that have already been published in the simulation section, which shows that

every method has its own advantages and disadvantages. EKF1 is the most accurate method during steady-state conditions, CKF is in the second position with $TVE = 0.06$, and EKF2 is the least accurate with $TVE = 0.09\%$. All five non-linear Kalman filters show the same bandwidth when amplitude and phase have sinusoidal variation. TVE is approximately 0.5% for all filters. Overshoot of EKF2 is the least one (3.2%) when there is an amplitude-step change in the input signal, and EKF1 has the most significant overshoot when there is a phase-step change in the input signal. The longest response time is related to EKF2 (7.6 ms), and the shortest is for CKF (5.6 ms) during amplitude-step change. GHKF should be the last solution when there are many states or samples in the input signal. CKF, EKF1, and EKF2 show acceptable computation time when the sample number rises. CKF is the most accurate method in a high level of noise infiltration, and EKF1 is the best in low noise level special $SNR > 60$ dB. Finally, CKF has better performance than the six dynamic phasor estimation methods extracted from published papers. TVE of CKF is 0.1101%, and simulation time is 0.6148 ms. Although EKF1 has a lower computation burden (0.5491 ms), the estimation accuracy (0.1303%) is higher.

VI. FUTURE WORK

Phasor estimation is a crucial concept in the operation of a power system. More efficient estimation methods will improve monitoring and protection of electrical system power. Efficiency will be increased by higher speed, lower computation burden, and higher stability. Digital signal processing (DSP) and electrical power engineering are two wings that facilities this route. The electrical power system is becoming more complex and needs more sophisticated DSP methods. Kalman filter with zero delays in the estimation process is a promising method, and new methods (or augmented methods) should be applied in measured signals in a complex power system. With progress in the integration of renewable energies with converter-based technologies, new phenomena are created in the power system that a better observer can extract. We are looking for a DSP method that can give accurate estimates during transient conditions in the monitoring and protection field. A smoother estimation during severe fault conditions in power systems is an interesting direction for electrical power engineers. It is worth noting that besides the noisy data (lack of quality), the PMU-based monitoring is usually contaminated with communication failure (unavailability), which is not tackled in this paper. However, this will be a hot topic in the future with much more amount of data and communication failure such as GPS unavailability or even fictitious data by a cyber-attack. This issue is not answered in this paper because, in this paper, the focus was on the accuracy of dynamic phasor estimates by non-linear Kalman filters. However, we are working on big data and blockchain applications in PMU-based monitoring systems in an electrical power system to address these issues.

REFERENCES

- [1] P. M. De Oliveira-De Jesus, N. A. Rodriguez, D. F. Celeita, and G. A. Ramos, "PMU-based system state estimation for multigrounded distribution systems," *IEEE Trans. Power Syst.*, vol. 36, no. 2, pp. 1071–1081, Mar. 2021.
- [2] M. Cui, J. Wang, J. Tan, A. R. Florita, and Y. Zhang, "A novel event detection method using PMU data with high precision," *IEEE Trans. Power Syst.*, vol. 34, no. 1, pp. 454–466, Jan. 2019.
- [3] J. Zhao and G. Zhang, "A robust Prony method against synchrophasor measurement noise and outliers," *IEEE Trans. Power Syst.*, vol. 32, no. 3, pp. 2484–2486, May 2017.
- [4] K. E. Martin *et al.*, "Exploring the IEEE standard C37.118–2005 synchrophasors for power systems," *IEEE Trans. Power Del.*, vol. 23, no. 4, pp. 1805–1811, Oct. 2008.
- [5] A. G. Phadke and J. S. Thorp, *Synchronized Phasor Measurements and Their Applications*. Springer, 2008.
- [6] T. H. Demiray, "Simulation of power system dynamics using dynamic phasor models," Ph.D. dissertation, 2008.
- [7] P. Mattavelli, G. C. Verghes, and A. M. Stankovic, "Phasor dynamics of thyristor-controlled series capacitor systems," *IEEE Trans. Power Syst.*, vol. 12, no. 3, pp. 1259–1267, Aug. 1997.
- [8] J. Khodaparast and M. Khederzadeh, "Least square and Kalman based methods for dynamic phasor estimation: A review," *Protection Control Mod. Power Syst.*, vol. 2, no. 1, p. 1, Dec. 2017.
- [9] V. Choqueuse, A. Belouchrani, F. Auger, and M. Benbouzid, "Frequency and phasor estimations in three-phase systems: Maximum likelihood algorithms and theoretical performance," *IEEE Trans. Smart Grid*, vol. 10, no. 3, pp. 3248–3258, May 2019.
- [10] B. Jafarpisheh, S. M. Madani, and S. Jafarpisheh, "Improved DFT-based phasor estimation algorithm using down-sampling," *IEEE Trans. Power Del.*, vol. 33, no. 6, pp. 3242–3245, Dec. 2018.
- [11] S. Affijulla and P. Tripathy, "Development of dictionary-based phasor estimator suitable for p-class phasor measurement unit," *IEEE Trans. Instrum. Meas.*, vol. 67, no. 11, pp. 2603–2615, Nov. 2018.
- [12] S. Nanda and P. K. Dash, "A Gauss–Newton ADALINE for dynamic phasor estimation of power signals and its FPGA implementation," *IEEE Trans. Instrum. Meas.*, vol. 67, no. 1, pp. 45–56, Jan. 2018.
- [13] J. Ren and M. Kezunovic, "Real-time power system frequency and phasors estimation using recursive wavelet transform," *IEEE Trans. Power Del.*, vol. 26, no. 3, pp. 1392–1402, Jul. 2011.
- [14] A. T. Munoz and J. A. de la O. Serna, "Shanks' method for dynamic phasor estimation," *IEEE Trans. Instrum. Meas.*, vol. 57, no. 4, pp. 813–819, Apr. 2008.
- [15] *IEEE Standard for Synchrophasor Measurements for Power Systems*, IEEE Standard C37.118.1-2011 (Revision IEEE Std C37.118-2005), Dec. 2011, pp. 1–61.
- [16] M. McDonald *et al.*, "Power swing and out-of-step considerations on transmission lines," in *Proc. IEEE PSRC WG D*, vol. 6, 2005, p. 2005. [Online]. Available: https://www.ewh.ieee.org/r6/san_francisco/pes/pes_pdf/OutOfStep/PowerSwingOOS.pdf
- [17] J. A. de la O. Serna, "Synchrophasor estimation using Prony's method," *IEEE Trans. Instrum. Meas.*, vol. 62, no. 8, pp. 2119–2128, Aug. 2013.
- [18] D.-G. Lee, S.-H. Kang, and S.-R. Nam, "Phasor estimation algorithm based on the least square technique during CT saturation," *J. Electr. Eng. Technol.*, vol. 6, no. 4, pp. 459–465, Jul. 2011.
- [19] X. Jin, F. Wang, and Z. Wang, "A dynamic phasor estimation algorithm based on angle-shifted energy operator," *Sci. China Technol. Sci.*, vol. 56, no. 6, pp. 1322–1329, Jun. 2013.
- [20] J. A. de la O. Serna and J. Rodriguez-Maldonado, "Instantaneous oscillating phasor estimates with Taylor^K-Kalman filters," *IEEE Trans. Power Syst.*, vol. 26, no. 4, pp. 2336–2344, Apr. 2011.
- [21] J. A. de la O. Serna and J. Rodriguez-Maldonado, "Taylor–Kalman–Fourier filters for instantaneous oscillating phasor and harmonic estimates," *IEEE Trans. Instrum. Meas.*, vol. 61, no. 4, pp. 941–951, Apr. 2012.
- [22] J. A. O. de la Serna, "Dynamic phasor estimates for power system oscillations," *IEEE Trans. Instrum. Meas.*, vol. 56, no. 5, pp. 1648–1657, Oct. 2007.
- [23] I. Kamwa, A. K. Pradhan, and G. Joos, "Adaptive phasor and frequency-tracking schemes for wide-area protection and control," *IEEE Trans. Power Del.*, vol. 26, no. 2, pp. 744–753, Apr. 2011.
- [24] S.-H. Kang, D.-G. Lee, S.-R. Nam, P. A. Crossley, and Y.-C. Kang, "Fourier transform-based modified phasor estimation method immune to the effect of the DC offsets," *IEEE Trans. Power Del.*, vol. 24, no. 3, pp. 1104–1111, Jul. 2009.
- [25] A. G. Phadke and B. Kaszteny, "Synchronized phasor and frequency measurement under transient conditions," *IEEE Trans. Power Del.*, vol. 24, no. 1, pp. 89–95, Jan. 2009.
- [26] P. K. Dash, K. R. Krishnanand, and R. K. Patnaik, "Dynamic phasor and frequency estimation of time-varying power system signals," *Int. J. Electr. Power Energy Syst.*, vol. 44, no. 1, pp. 971–980, Jan. 2013.
- [27] M. A. Platas-Garza, J. Platas-Garza, and J. A. O. de la Serna, "Dynamic phasor and frequency estimates through maximally flat differentiators," *IEEE Trans. Instrum. Meas.*, vol. 59, no. 7, pp. 1803–1811, Jul. 2010.
- [28] J. A. O. Serna, "Phasor estimation from phasorlets," *IEEE Trans. Instrum. Meas.*, vol. 54, no. 1, pp. 134–143, Feb. 2005.
- [29] J. A. D. L. O. Serna and K. E. Martin, "Improving phasor measurements under power system oscillations," *IEEE Trans. Power Syst.*, vol. 18, no. 1, pp. 160–166, Feb. 2003.
- [30] J. A. O. de la Serna, "Reducing the error in phasor estimates from phasorlets in fault voltage and current signals," *IEEE Trans. Instrum. Meas.*, vol. 56, no. 3, pp. 856–866, Jun. 2007.
- [31] H. M. Al-Hamadi and K. M. El-Naggar, "Measurement of synchronous machine parameters using Kalman filter based fuzzy logic estimator," *Measurement*, vol. 43, no. 10, pp. 1327–1335, Dec. 2010.
- [32] R. Faragher, "Understanding the basis of the Kalman filter via a simple and intuitive derivation," *IEEE Signal Process. Mag.*, vol. 29, no. 5, pp. 128–132, Sep. 2012.
- [33] P. F. Ribeiro, C. A. Duque, P. M. Ribeiro, and A. S. Cerqueira, *Power Systems Signal Processing for Smart Grids*. Hoboken, NJ, USA: Wiley, 2013.
- [34] Z. Aydogmus and O. Aydogmus, "A comparison of artificial neural network and extended Kalman filter based sensorless speed estimation," *Measurement*, vol. 63, pp. 152–158, Mar. 2015.
- [35] B. F. La Scala and R. R. Bitmead, "Design of an extended Kalman filter frequency tracker," *IEEE Trans. Signal Process.*, vol. 44, no. 3, pp. 739–742, 1996.
- [36] B. F. La Scala and R. R. Bitmead, "Design of an extended Kalman filter frequency tracker," in *Proc. IEEE Int. Conf. Acoust., Speech Signal Process. (ICASSP)*, vol. 3, Apr. 1994, p. III-525.
- [37] P. M. Ramos and A. C. Serra, "Comparison of frequency estimation algorithms for power quality assessment," *Measurement*, vol. 42, no. 9, pp. 1312–1317, Nov. 2009.
- [38] M. Bertocco, G. Frigo, G. Giorgi, and C. Narduzzi, "Frequency tracking for efficient phasor measurement based on a CSTFM model," in *Proc. IEEE Int. Workshop Appl. Meas. Power Syst. (AMPS)*, Sep. 2015, pp. 84–89.
- [39] D. Fontanelli, D. Macii, and D. Petri, "Dynamic synchrophasor estimation using smoothed Kalman filtering," in *Proc. IEEE Int. Instrum. Meas. Technol. Conf.*, May 2016, pp. 1–6.
- [40] H. Hajimolahoseini, M. R. Taban, and H. Soltanian-Zadeh, "Extended Kalman filter frequency tracker for nonstationary harmonic signals," *Measurement*, vol. 45, no. 1, pp. 126–132, Jan. 2012.
- [41] A. K. Pradhan, "Voltage phasor estimation using complex linear Kalman filter," in *Proc. 8th IEE Int. Conf. Develop. Power Syst. Protection*, vol. 1, 2004, pp. 24–27.
- [42] P. K. Dash, S. Hasan, and B. K. Panigrahi, "A hybrid unscented filtering and particle swarm optimization technique for harmonic analysis of nonstationary signals," *Measurement*, vol. 43, no. 10, pp. 1447–1457, Dec. 2010.
- [43] H. Novanda, P. Regulski, F. M. González-Longatt, and V. Terzija, "Unscented Kalman filter for frequency and amplitude estimation," in *Proc. IEEE Trondheim PowerTech*, Jun. 2011, pp. 1–6.
- [44] H. Novanda, P. Regulski, F. González-Longatt, and V. Terzija, "Phasor estimation considering DC component using UKF," in *Proc. Int. Conf. Adv. Power Syst. Automat. Protection*, vol. 3, Oct. 2011, pp. 2438–2442.
- [45] I. Arasaratnam, S. Haykin, and R. J. Elliott, "Discrete-time nonlinear filtering algorithms using Gauss–Hermite quadrature," *Proc. IEEE*, vol. 95, no. 5, pp. 953–977, May 2007.
- [46] S. Särkkä, *Recursive Bayesian Inference on Stochastic Differential Equations*. Helsinki Univ. Technology, 2006.
- [47] I. Arasaratnam and S. Haykin, "Cubature Kalman filters," *IEEE Trans. Autom. Control*, vol. 54, no. 6, pp. 1254–1269, Jun. 2009.
- [48] H. Pesonen and R. Piché, "Cubature-based Kalman filters for positioning," in *Proc. 7th Workshop Positioning, Navigat. Commun.*, Mar. 2010, pp. 45–49.
- [49] K. Salahshoor, M. Mosallaei, and M. Bayat, "Centralized and decentralized process and sensor fault monitoring using data fusion based on adaptive extended Kalman filter algorithm," *Measurement*, vol. 41, no. 10, pp. 1059–1076, 2008.

- [50] Z. Lai, Y. Lei, S. Zhu, Y.-L. Xu, X.-H. Zhang, and S. Krishnaswamy, "Moving-window extended Kalman filter for structural damage detection with unknown process and measurement noises," *Measurement*, vol. 88, pp. 428–440, Jun. 2016.
- [51] J. Pomárico-Franquíz, S. H. Khan, and Y. S. Shmaliy, "Combined extended FIR/Kalman filtering for indoor robot localization via triangulation," *Measurement*, vol. 50, pp. 236–243, Apr. 2014.
- [52] D.-J. Jwo and T.-S. Cho, "Critical remarks on the linearised and extended Kalman filters with geodetic navigation examples," *Measurement*, vol. 43, no. 9, pp. 1077–1089, Nov. 2010.
- [53] K. Xiong, H. Y. Zhang, and C. Chan, "Performance evaluation of UKF-based nonlinear filtering," *Automatica*, vol. 42, no. 2, pp. 261–270, 2006.
- [54] S. J. Julier and J. K. Uhlmann, "Unscented filtering and nonlinear estimation," *Proc. IEEE*, vol. 92, no. 3, pp. 401–422, Mar. 2004.
- [55] Z. Jiang, Q. Song, Y. He, and J. Han, "A novel adaptive unscented Kalman filter for nonlinear estimation," in *Proc. 46th IEEE Conf. Decis. Control*, Dec. 2007, pp. 4293–4298.
- [56] K. Ito and K. Xiong, "Gaussian filters for nonlinear filtering problems," *IEEE Trans. Autom. Control*, vol. 45, no. 5, pp. 910–927, May 2000.
- [57] H. H. Afshari, S. A. Gadsden, and S. Habibi, "Gaussian filters for parameter and state estimation: A general review of theory and recent trends," *Signal Process.*, vol. 135, pp. 218–238, Jun. 2017.
- [58] A. J. Haug, *Bayesian Estimation and Tracking: A Practical Guide*. Hoboken, NJ, USA: Wiley, 2012.
- [59] R. Radhakrishnan, A. K. Singh, S. Bhaumik, and N. K. Tomar, "Multiple sparse-grid Gauss–Hermite filtering," *Appl. Math. Model.*, vol. 40, nos. 7–8, pp. 4441–4450, 2016.
- [60] D. Wang, H. Lv, and J. Wu, "Augmented cubature Kalman filter for nonlinear RTK/MIMU integrated navigation with non-additive noise," *Measurement*, vol. 97, pp. 111–125, Feb. 2017.
- [61] Q. Chen, W. Wang, and C. Yin, "Distributed state estimations based on cubature Kalman filtering," in *Proc. Chin. Control Decis. Conf. (CCDC)*, May 2016, pp. 3384–3389.
- [62] K. Pakki, B. Chandra, D.-W. Gu, and I. Postlethwaite, "Cubature information filter and its applications," in *Proc. Amer. Control Conf.*, Jun. 2011, pp. 3609–3614.
- [63] J. Khodaparast and M. Khederzadeh, "Three-phase fault detection during power swing by transient monitor," *IEEE Trans. Power Syst.*, vol. 30, no. 5, pp. 2558–2565, Sep. 2015.
- [64] C. Pang and M. Kezunovic, "Fast distance relay scheme for detecting symmetrical fault during power swing," *IEEE Trans. Power Del.*, vol. 25, no. 4, pp. 2205–2212, Oct. 2010.
- [65] J. G. Rao and A. K. Pradhan, "Differential power-based symmetrical fault detection during power swing," *IEEE Trans. Power Del.*, vol. 27, no. 3, pp. 1557–1564, Jul. 2012.
- [66] S. Lotfifard, J. Faiz, and M. Kezunovic, "Detection of symmetrical faults by distance relays during power swings," *IEEE Trans. Power Del.*, vol. 25, no. 1, pp. 81–87, Jan. 2010.
- [67] B. Mahamedi and J. G. Zhu, "A novel approach to detect symmetrical faults occurring during power swings by using frequency components of instantaneous three-phase active power," *IEEE Trans. Power Del.*, vol. 27, no. 3, pp. 1368–1376, Jul. 2012.
- [68] *IEEE Standard for Synchrophasor Measurements for Power Systems*, Standard C37. 118.1-2011, IEEE Standard Association, 2011.
- [69] *118-1: Synchrophasor for Power System-Measurements*, IEEE Standard P60255-118-1, 2018.
- [70] A. T. Munoz and J. A. de la O. Serna, "Shanks' method for dynamic phasor estimation," *IEEE Trans. Instrum. Meas.*, vol. 57, no. 4, pp. 813–819, Apr. 2008.
- [71] J. Rodriguez, "Instantaneous oscillating phasor estimates with Taylor^K-Kalman filters," Ph.D. dissertation, 2011.
- [72] J. Liu, F. Ni, J. Tang, F. Ponci, and A. Monti, "A modified Taylor–Kalman filter for instantaneous dynamic phasor estimation," in *Proc. 3rd IEEE PES Innov. Smart Grid Technol. Eur. (ISGT Europe)*, Oct. 2012, pp. 1–7.



JALAL KHODAPARAST received the bachelor's and master's degrees in science from the Shahrood University of Technology, in 2009 and 2011, respectively. He is currently pursuing the Ph.D. degree with Shahid Beheshti University. He defended his Ph.D. thesis, in 2017. His thesis was related to dynamic phenomena in a power system, protection, and FACTS. He did a 12-month postdoctoral research scholarship from ERCIM "Alain Bensoussan Fellowship Programme" at NTNU. He worked on monitoring of modern power system at PMU. Then, he worked on the stability of large-scale power system dominated by power electronic technologies in his second postdoctoral position at NTNU. He worked on PSS and power quality in B.Sc. and M.Sc. degrees. He is currently an Associate Professor with the Department of Electrical Engineering, IT and Cybernetic, University of South-Eastern Norway (USN), Porsgrunn, Norway. His research interests include power system stability, monitoring of power systems, PMU, integration of renewable energies to the power systems, application of signal processing in power systems, HVDC, and FACTS devices.

• • •